

# MicroRNA-30 family members regulate calcium/calcineurin signaling in podocytes

Junnan Wu, Chunxia Zheng, Xiao Wang, Shifeng Yun, Yue Zhao, Lin Liu, Yuqiu Lu, Yuting Ye, Xiaodong Zhu, Changming Zhang, Shaolin Shi, and Zhihong Liu

National Clinical Research Center of Kidney Diseases, Jinling Hospital, Nanjing University School of Medicine, Nanjing, China.

Calcium/calcineurin signaling is critical for normal cellular physiology. Abnormalities in this pathway cause many diseases, including podocytopathy; therefore, understanding the mechanisms that underlie the regulation of calcium/calcineurin signaling is essential. Here, we showed that critical components of calcium/calcineurin signaling, including *TRPC6*, *PPP3CA*, *PPP3CB*, *PPP3R1*, and *NFATC3*, are the targets of the microRNA-30 family (miR-30s). We found that these 5 genes are highly expressed as mRNA, but the level of the proteins is low in normal podocytes. Conversely, protein levels were markedly elevated in podocytes from rats treated with puromycin aminonucleoside (PAN) and from patients with focal segmental glomerulosclerosis (FSGS). In both FSGS patients and PAN-treated rats, miR-30s were downregulated in podocytes. In cultured podocytes, PAN or a miR-30 sponge increased *TRPC6*, *PPP3CA*, *PPP3CB*, *PPP3R1*, and *NFATC3* expression; calcium influx; intracellular  $Ca^{2+}$  concentration; and calcineurin activity. Moreover, *NFATC3* nuclear translocation, synaptopodin degradation, integrin  $\beta 3$  (ITGB3) activation, and actin fiber loss, which are downstream of calcium/calcineurin signaling, were induced by miR-30 reduction but blocked by the calcineurin inhibitor FK506. Podocyte-specific expression of the miR-30 sponge in mice increased calcium/calcineurin pathway component protein expression and calcineurin activity. The mice developed podocyte foot process effacement and proteinuria, which were prevented by FK506. miR-30s also regulated calcium/calcineurin signaling in cardiomyocytes. Together, our results identify miR-30s as essential regulators of calcium/calcineurin signaling.

## Introduction

Podocyte injury and loss have emerged as a central pathological mechanism underlying glomerular injury and sclerosis (1). Although multiple signaling pathways have been implicated in podocyte injury (2, 3), the mechanism underlying podocyte injury remains incompletely understood. Studies have demonstrated that miRs are necessary for podocyte homeostasis, as demonstrated by the effects of a selective Dicer deletion on mouse podocytes (4–6). More recently, several microRNAs (miRs), including miR-193a (7), miR-29a (8), and the miR-30 family (miR-30s) (9, 10), have been implicated in podocyte injury.

The miR-30 family is evolutionarily conserved and consists of 5 members, miR-30a through miR-30e. We have previously found that miR-30 family members are abundantly expressed in podocytes but are markedly downregulated upon podocyte injury and that miR-30 downregulation facilitates podocyte apoptosis (9). In addition, we have shown that miR-30 downregulation can induce actin fiber disruption and podocyte loss (9), suggesting that miR-30s are involved in podocyte actin fiber and cytoskeletal stability via an undetermined mechanism.

Actin fiber remodeling and cytoskeletal damage to podocytes are frequently observed in various glomerular diseases, and these events lead to foot process effacement, glomerular fil-

tration barrier damage, and podocyte detachment (11, 12). Many studies have been performed to determine the mechanisms underlying podocyte cytoskeletal damage (13), and calcium/calcineurin signaling is known to play a critical role in podocyte cytoskeletal injury (14). Calcium/calcineurin signaling has also been implicated in podocyte apoptosis (15–17).

Calcium/calcineurin signaling is initiated by the movement of  $Ca^{2+}$  from the extracellular space into cells. The transient receptor potential cation channel (TRPC) family, which consists of 6 members (TRPC1 through TRPC6), functions as a  $Ca^{2+}$  transporter. After entry into the cells,  $Ca^{2+}$  binds to calcineurin and activates its phosphatase activity. Calcineurin is composed of an  $\alpha$ -catalytic subunit and a  $\beta$ -regulatory subunit. The  $\alpha$ -catalytic subunit gene family consists of 3 members (*PPP3CA*, *PPP3CB*, and *PPP3CC*), and the  $\beta$ -regulatory subunit family consists of 2 members (*PPP3R1* and *PPP3R2*) (18–20). Activated calcineurin dephosphorylates cytoplasmic nuclear factor of activated T cell (NFATC) family members, resulting in their translocation to the nucleus, where they function as transcription factors to regulate gene expression. Calcineurin signaling has been implicated in many cellular processes, including T cell activation (21), apoptosis (22, 23), cardiomyocyte hypertrophy (24–28), and neural dysfunction (29, 30). Moreover, many studies have demonstrated the role of calcium/calcineurin signaling in podocyte injury. For instance, a gain-of-function mutation in *TRPC6* results in increased cellular  $Ca^{2+}$  levels and aberrant  $Ca^{2+}$  signaling in podocytes, leading to podocyte injury and focal segmental glomerulosclerosis (FSGS) (31, 32). Upon podocyte injury, calcineurin

**Authorship note:** Junnan Wu and Chunxia Zheng contributed equally to this work.

**Conflict of interest:** The authors have declared that no conflict of interest exists.

**Submitted:** January 20, 2015; **Accepted:** August 27, 2015.

**Reference information:** *J Clin Invest*. 2015;125(11):4091–4106. doi:10.1172/JCI81061.

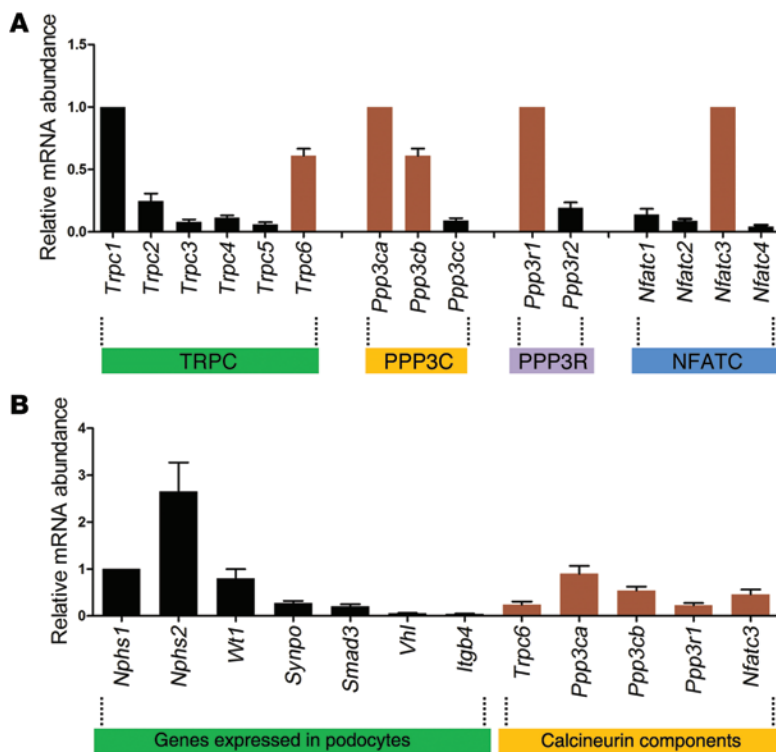


**Figure 1.** *Trpc6*, *Ppp3ca*, *Ppp3cb*, *Ppp3r1*, and *Nfatc3* are the family members expressed at high mRNA levels in mouse podocytes. (A) qPCR analysis of purified mouse podocytes demonstrating the relative abundances of all family members in mouse podocytes and showing that 5 genes are the predominantly expressed members of these families at the mRNA level ( $n = 6$ ). (B) Comparison of the mRNA abundance of these 5 genes with that of other genes known to be highly expressed or to function in podocytes ( $n = 6$ ).

to downstream signaling, suggesting that miR-30s might strongly inhibit calcium/calcineurin signaling.

mRNA levels of *TRPC6*, *PPP3CA*, *PPP3CB*, *PPP3R1*, and *NFATC3* are high, but those of other family members are low in both mouse podocytes and human glomeruli. The *TRPC*, *PPP3C*, *PPP3R*, and *NFATC* gene families consist of 2 to 6 members that may be functionally redundant. To determine which members of these families are expressed and function in podocytes, we performed quantitative PCR (qPCR) analysis of their mRNA expression in mouse podocytes. To isolate mouse podocytes, we crossed Gt(ROSA)26Sor<sup>tm4(ACTB-tdTomato, eGFP)</sup>Luo mice (34) with *NPHS2-Cre* transgenic mice (35) to label podocytes with EGFP (Supplemental Figure 1A) and isolated the podocytes (Supplemental Figure 1, B–D). qPCR

dephosphorylates synaptopodin (SYNPO), an actin stabilizer in podocytes, resulting in SYNPO degradation and consequent cytoskeletal rearrangement and proteinuria (33). Moreover, calcium/calcineurin signaling-induced NFATC activation causes podocyte injury and glomerulosclerosis (16, 17).

Although the role of calcium/calcineurin signaling in podocyte injury is well documented, little is known about its regulation, especially regulation of the expression of its essential components. Given our our findings that miR-30 loss of function causes podocyte cytoskeletal damage and that the gene encoding calcium/calcineurin signaling components are enriched among the list of predicted miR-30 targets, we hypothesized that miR-30s may inhibit calcium/calcineurin signaling and that miR-30 down-regulation may result in its activation, leading to podocyte injury. We tested this hypothesis in the present study.

## Results

*miR-30s are predicted to inhibit calcium/calcineurin signaling.* To explore the functions of miR-30s, we performed Ingenuity Pathway Analysis (IPA) on the predicted targets of miR-30s (www.targetscan.org) and found that the genes that are associated with calcium/calcineurin signaling are highly enriched in the list of predicted miR-30 target genes (Supplemental Tables 1 and 2; supplemental material available online with this article; doi:10.1172/JCI81061DS1). As mentioned above, some of these Ca<sup>2+</sup>-associated genes, including *TRPC6* of the *TRPC* family, *PPP3CA* and *PPP3CB* of the calcineurin catalytic subunit (*PPP3C*) family, *PPP3R1* of the calcineurin regulatory subunit (*PPP3R*) family, and *NFATC3* of the *NFATC* family, are known to be involved in podocyte injury. Interestingly, these 5 genes function at different steps of this signaling pathway, from Ca<sup>2+</sup> entry

analyses of all members of the 4 families revealed that the 5 members of predicted miR-30 targets, *Trpc6*, *Ppp3ca*, *Ppp3cb*, *Ppp3r1*, and *Nfatc3*, were dominantly expressed in the podocytes compared with the non-miR-30 targets, except for *Trpc1* (Figure 1A). In addition, the mRNA levels of *Trpc6*, *Ppp3ca*, *Ppp3cb*, *Ppp3r1*, and *Nfatc3* were equivalent to those of nephrin (*Nphs1*), podocin (*Nphs2*), *Wt1*, and SYNPO (*Synpo*), which are podocyte markers that are known to be highly expressed, and were higher than those of *Smad3*, *Vhl* and *Igfb4* (Figure 1B), which are known to be expressed and to function in podocytes (36–38).

We also examined the mRNA levels of these genes in human glomeruli according to their signal intensities indicated in the NCBI's Gene Expression Omnibus (GEO) datasets microarray database (www.ncbi.nlm.nih.gov/gds/) (39) (Supplemental Table 3). We found an expression pattern similar to that in mice (Supplemental Figure 2A), and qPCR analysis confirmed these results (Supplemental Figure 2B). Additionally, this expression pattern was recapitulated in an immortalized human podocyte cell line that we used in the present study (Supplemental Figure 2C).

*TRPC6*, *PPP3CA*, *PPP3CB*, *PPP3R1*, and *NFATC3* protein levels are low in rat podocytes but are upregulated in the podocytes of puromycin aminonucleoside-treated rats, and this upregulation is prevented by exogenous miR-30a or glucocorticoids. We have previously shown that miR-30s are downregulated in the podocytes of puromycin aminonucleoside-treated (PAN-treated) rats (9). Therefore, the protein levels of *TRPC6*, *PPP3CA*, *PPP3CB*, *PPP3R1*, and *NFATC3* would be elevated if these genes are genuine miR-30 targets. IHC analysis of the kidneys from the untreated and PAN-treated rats revealed that these 5 proteins were either undetectable or were expressed at very low levels in normal podocytes (Supplemental Figure 3A). The low protein lev-

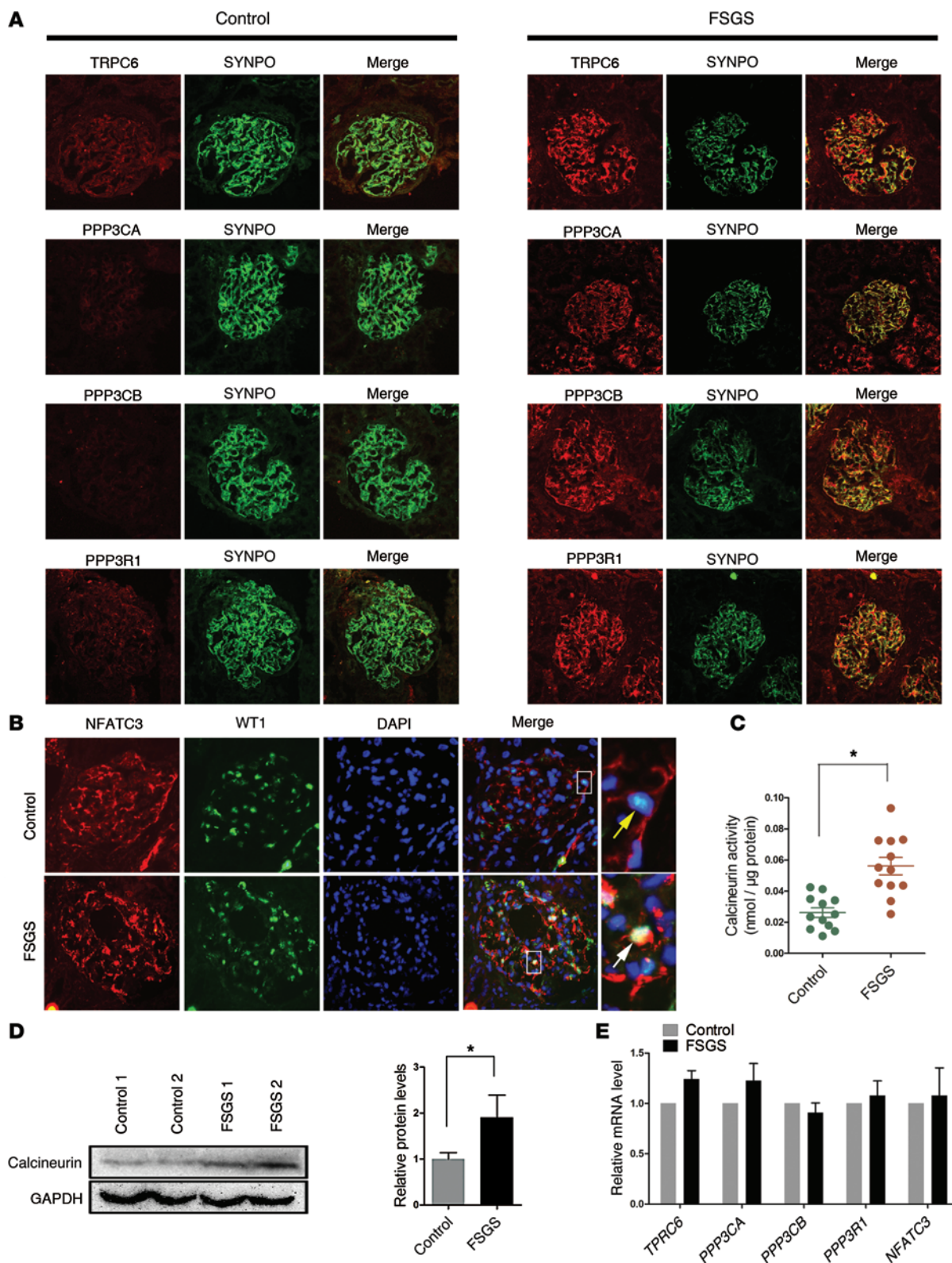


**Figure 2. TRPC6, PPP3CA, PPP3CB, PPP3R1, and NFATC3 protein expression in human podocytes from control subjects and patients with FSGS.** (A) IF staining demonstrated that the protein levels of these genes are low in normal podocytes but are significantly upregulated in the podocytes of patients with FSGS. Original magnification,  $\times 20$ . Representative images of 4 subjects are shown for each group. (B) IF staining for NFATC3 in the same tissues revealed upregulation and nuclear accumulation of NFATC3 (original magnification,  $\times 20$ , as shown by colocalization with WT1; insets, original magnification,  $\times 100$ ) in the podocytes of FSGS patients. Representative images of 4 subjects are shown for each group. (C) Calcineurin activity in the glomeruli of controls and FSGS patients ( $n = 12$  in each group). Two-tailed Student's  $t$  test,  $*P < 0.05$ . (D) Immunoblotting for calcineurin in glomeruli isolated from controls or FSGS patients ( $n = 8$  in each group). Parallel gels were run for calcineurin and GAPDH. Quantification of the gels is shown on the right. Two-tailed Student's  $t$  test,  $*P < 0.05$ . (E) qPCR analysis showing that the mRNA levels of these genes in the glomeruli were not different between FSGS patients and controls ( $n = 6$  in each group).

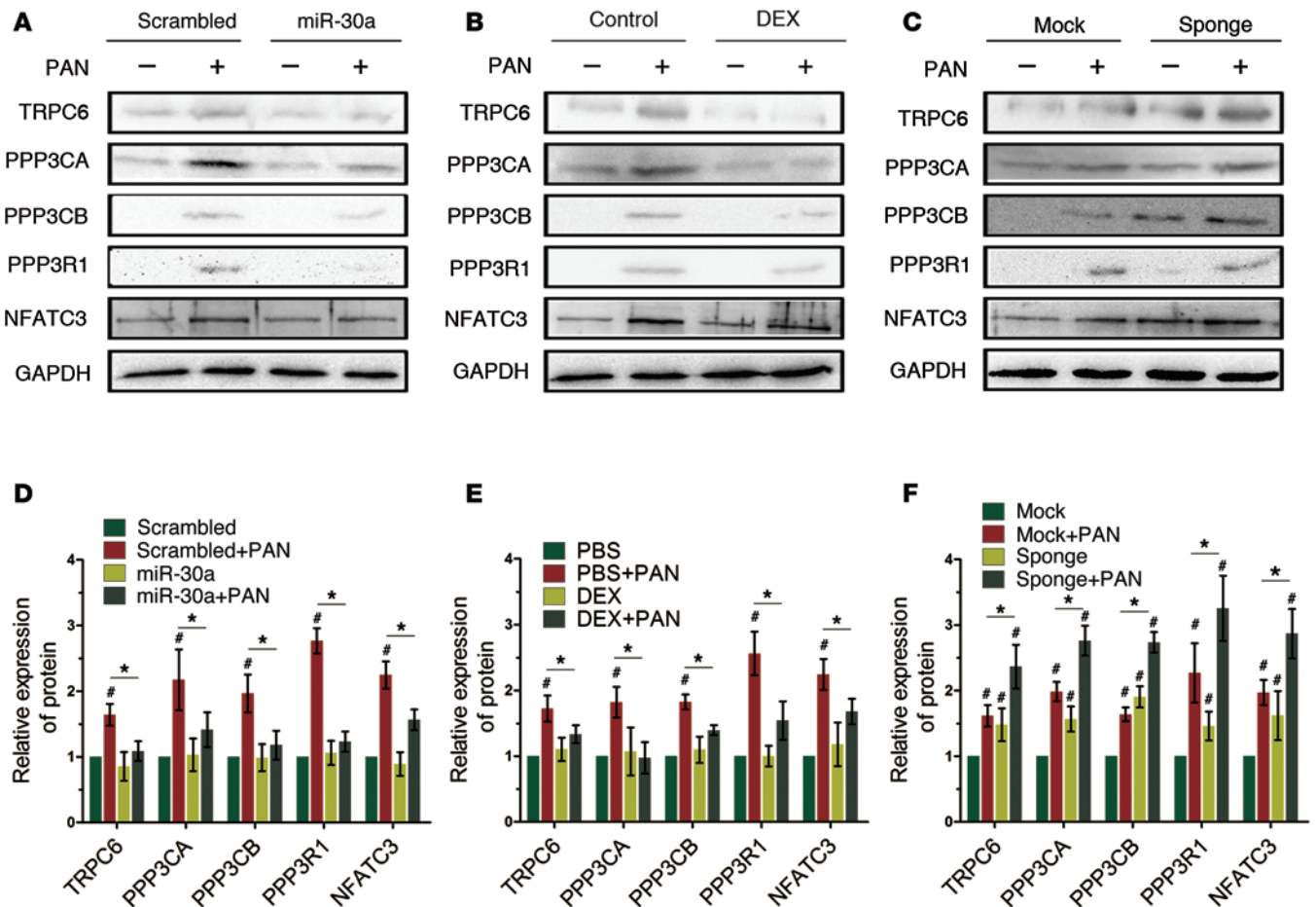


**Figure 3. miR-30s regulate the expression of TRPC6, PPP3CA, PPP3CB, PPP3R1, and NFATC3 proteins in cultured human podocytes.** (A and B) Immunoblots showing that miR-30a overexpression (A) or DEX (B) blocked the PAN-induced upregulation of these proteins. (C) A miR-30 sponge increased the expression of these proteins in the absence or presence of PAN. (D–F) Quantification of the results from A (D), B (E), and C (F). Parallel gels were run in each experiment for the indicated protein and GAPDH. Results are expressed as the mean ± SD of at least 3 experiments. One-way ANOVA, #*P* < 0.05 versus scrambled, PBS, or mock; \**P* < 0.05.

els of these factors, in contrast with their high mRNA levels, suggest that TRPC6, PPP3CA, PPP3CB, PPP3R1, and NFATC3 may be posttranscriptionally inhibited, presumably by miR-30s.

In contrast, these 5 proteins were significantly upregulated in podocytes from the PAN-treated rats, and the nuclear accumulation of the NFATC3 protein was clearly observed in these cells. Both the in vivo delivery of miR-30a and treatment with glucocorticoids (which are known to prevent PAN-induced miR-30 downregulation; ref. 9) prevented PAN-induced upregulation of these proteins (Supplemental Figure 3A). Immunoblotting with an antibody (anti-calceinurin) that recognized both the PPP3CA and PPP3CB proteins (calceinurin) further confirmed the upregulation of the 2 proteins (Supplemental Figure 3B). Consistently, calcineurin phosphatase activity was increased by PAN treatment and was mitigated by the in vivo delivery of miR-30a or glucocorticoid treatment (Supplemental Figure 3, C and D). These results further suggest that miR-30s target these 5 genes.

We next analyzed the mRNA levels of these genes in the glomeruli of PAN-treated rats and found that they were either unchanged (*Ppp3r1*) or were moderately increased (<2-fold), except for *Trpc6*, which displayed an approximately 6-fold

increase in expression compared with that detected in untreated control rats (Supplemental Figure 4). Apparently, the increased in mRNA levels of these genes did not account for their increased protein levels, further supporting the possibility that these genes are posttranscriptionally regulated.

We then performed qPCR to examine the expression of the non-miR-30 target members of the 4 families, including *Trpc1/2/3/4/5*, *Ppp3cc*, *Ppp3r2*, and *Nfatc1/2/4*, in the glomeruli of both normal and PAN-treated rats. However, no significant differences were observed (data not shown), demonstrating that TRPC6, PPP3CA, PPP3CB, PPP3R1, and NFATC3 are the family members that play major roles in the activation of calcium/calceinurin signaling in podocytes of PAN-treated rats.

*TRPC6, PPP3CA, PPP3CB, PPP3R1, and NFATC3 protein levels are also low in the podocytes of control subjects but are significantly elevated in those of FSGS patients.* We next examined the expression levels of TRPC6, PPP3CA, PPP3CB, PPP3R1, and NFATC3 in the podocytes/glomeruli of control subjects via immunofluorescence (IF) or IHC and found that they were either undetectable or expressed at low levels (Figure 2, A and B). Because *TRPC6*, *PPP3CA*, *PPP3CB*, *PPP3R1*, and *NFATC3* display high mRNA lev-

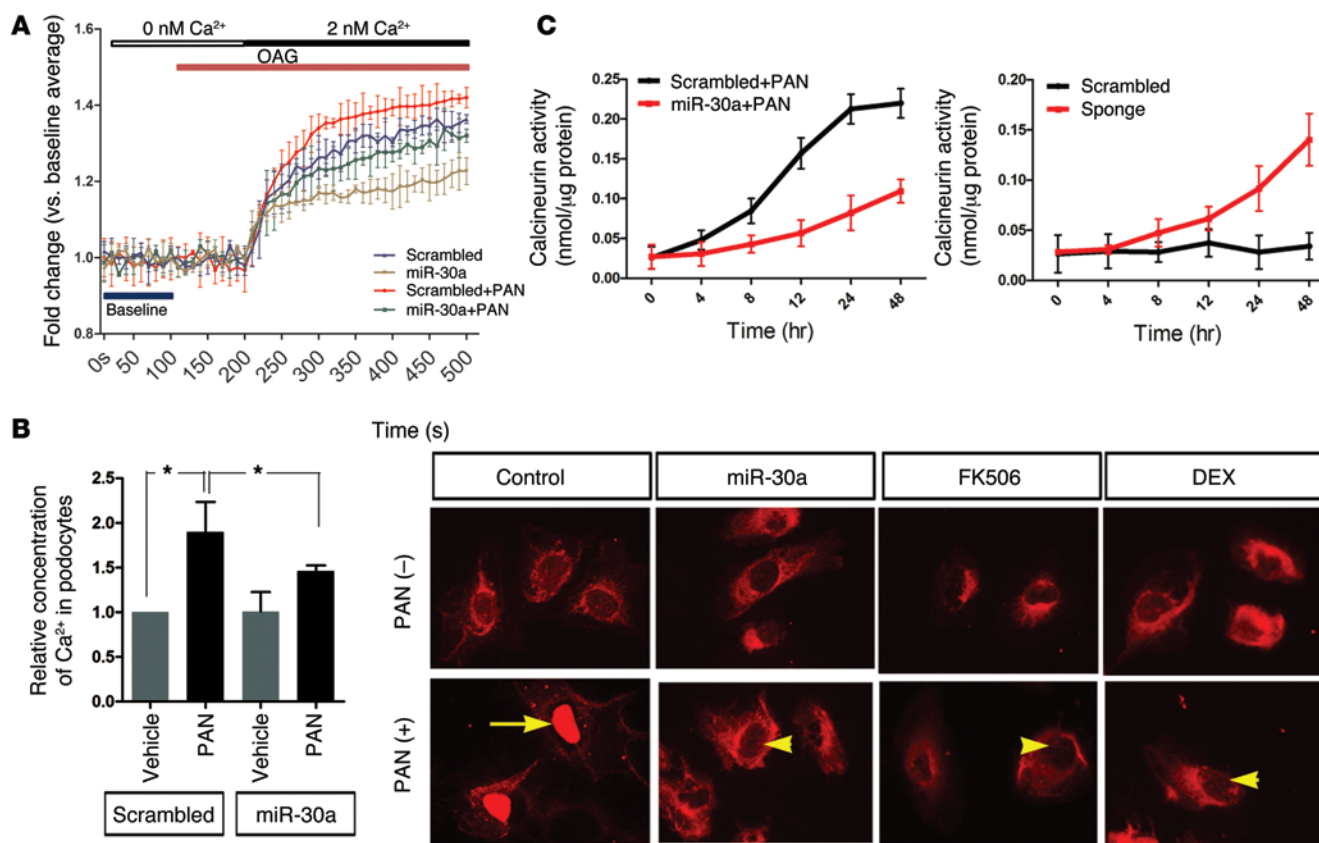


**Figure 4. miR-30s inhibit Ca<sup>2+</sup> entry and calcineurin signaling in cultured human podocytes.** (A) The Ca<sup>2+</sup> influx assay demonstrated that miR-30a overexpression attenuated the PAN-induced increase in Ca<sup>2+</sup> influx ( $n = 15\text{--}20$  cells). (B) miR-30a prevented PAN-induced intracellular Ca<sup>2+</sup> accumulation ( $n = 5$ ). Two-way ANOVA,  $*P < 0.05$ . (C) The calcineurin phosphatase activity assay showed that miR-30a overexpression prevented a PAN-induced increase in calcineurin activity (left panel), but miR-30 silencing using a miR-30 sponge was sufficient to increase calcineurin activity in the cultured podocytes (right panel) ( $n = 6$ ). (D) IF staining revealed that the nuclear translocation of NFATC3 was induced by PAN (arrow) but was prevented by FK506 or glucocorticoids (DEX) (arrowheads). Original magnification,  $\times 20$ . Representative images from 3 independent experiments are shown.

els in human podocytes/glomeruli, as demonstrated above, they should also be posttranscriptionally inhibited in human podocytes. In the podocytes of FSGS patients, these proteins were significantly upregulated, as demonstrated by both IF (Figure 2, A and B) and IHC (Supplemental Figure 5), and the nuclear accumulation of NFATC3 was apparent (Figure 2B). Calcineurin phosphatase activity in FSGS renal biopsies was also increased (Figure 2C), consistent with the increase in calcineurin protein (PPP3CA and PPP3CB) expression in the renal cortex of the FSGS patients, as demonstrated by immunoblotting using an anti-calcineurin antibody (Figure 2D). Importantly, *TRPC6*, *PPP3CA*, *PPP3CB*, *PPP3R1*, and *NFATC3* mRNA levels in the glomeruli were similar between the FSGS patients and control subjects (Figure 2E). Taken together, the results demonstrate that *TRPC6*, *PPP3CA*, *PPP3CB*, *PPP3R1*, and *NFATC3* protein expression levels are repressed in normal podocytes but are de-repressed in the podocytes of FSGS patients, in whom miR-30s are known to be downregulated, as demonstrated by our previous study (9) and this study (Supplemental Figure 6).

qPCR analysis of mRNA levels of the non-miR-30 target family members in the glomeruli of FSGS patients demonstrated that these mRNA expression levels were unchanged (data not shown), indicating that *TRPC6*, *PPP3CA*, *PPP3CB*, *PPP3R1*, and *NFATC3*

were the predominant family members responsible for calcium/calcineurin signaling activation in the podocytes of FSGS patients.

*TRPC6*, *PPP3CA*, *PPP3CB*, *PPP3R1*, and *NFATC3* are direct targets of miR-30s. *TRPC6*, *PPP3CA*, *PPP3CB*, *PPP3R1*, and *NFATC3* are predicted to be miR-30 targets (www.targetscan.org) (Supplemental Figure 7A). To experimentally demonstrate that miR-30s target these factors, we performed luciferase reporter assays. For each gene, we produced 2 constructs containing the luciferase coding region, followed by either the WT 3'-UTR or a 3'-UTR, in which the miR-30 site was mutated as indicated (Supplemental Figure 7A). When the cultured podocytes were cotransfected with the miR-30a-expressing plasmid, the construct containing the mutated miR-30 site displayed higher luciferase expression than did the WT miR-30 construct (Supplemental Figure 7, B-F). In contrast, when the miR-30 sponge plasmid was cotransfected, the WT reporter exhibited higher luciferase activity than did the mutant reporter (Supplemental Figure 7, B-F). Collectively, these results demonstrated that *TRPC6*, *PPP3CA*, *PPP3CB*, *PPP3R1*, and *NFATC3* are direct targets of miR-30s.

miR-30s regulate Ca<sup>2+</sup> influx, the intracellular Ca<sup>2+</sup> concentration, calcineurin phosphatase activity, and NFATC3 nuclear translocation in cultured podocytes. To functionally demonstrate that miR-30s control calcium/calcineurin signaling by regulating

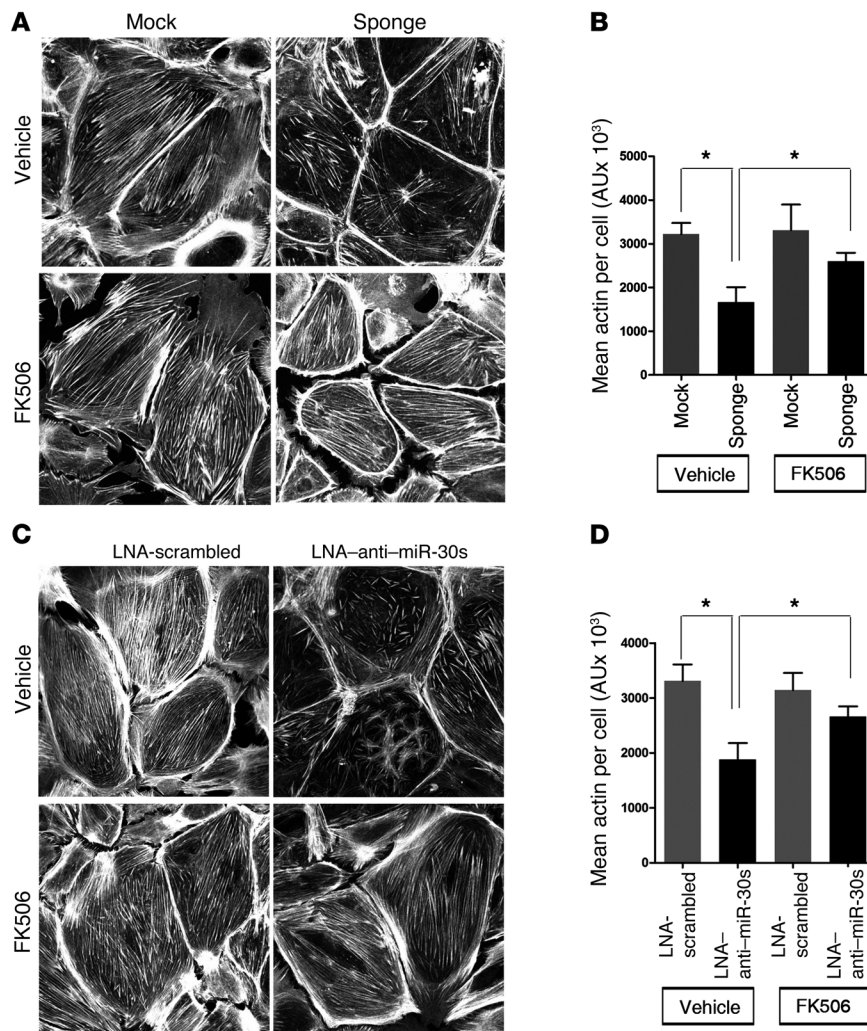


**Figure 5. miR-30 knockdown causes cytoskeletal damage to podocytes.** (A) Representative results of phalloidin staining showing that transfection with the miR-30 sponge resulted in loss of F-actin fibers from the cells and that this effect was prevented by FK506. Original magnification,  $\times 20$ . (B) Quantification of the results in A ( $n = 20$  cells). Two-way ANOVA,  $*P < 0.05$ . (C) Transfection of LNA-anti-miR-30s into cells similarly disrupted the F-actin fibers, an effect that was prevented by FK506. Original magnification,  $\times 20$ . (D) Quantification of the results in C ( $n = 20$  cells). Two-way ANOVA,  $*P < 0.05$ . LNA-Scr, scrambled control.

TRPC6, PPP3CA, PPP3CB, PPP3R1, and NFATC3, we overexpressed miR-30a in cultured podocytes. We found that miR-30a overexpression prevented the PAN-induced upregulation of these proteins (Figure 3, A and D). Glucocorticoid (dexamethasone [DEX]), which is known to prevent PAN-induced miR-30 downregulation (9), exerted a similar effect (Figure 3, B and E). However, miR-30 silencing using the miR-30 sponge increased the expression of these proteins, even in the absence of PAN (Figure 3, C and F). Neither miR-30a overexpression nor miR-30 sponge treatment altered the mRNA levels of the 5 genes (Supplemental Figure 8), indicating that miR-30s regulate the expression of these genes by inhibiting their translation in immortalized podocytes as well.

Consistently, miR-30a overexpression reduced  $\text{Ca}^{2+}$  influx (Figure 4A) and decreased the intracellular  $\text{Ca}^{2+}$  concentration in the PAN-treated podocytes (Figure 4B). Furthermore, miR-30 overexpression prevented a PAN-induced increase in calcineurin phosphatase activity in the podocytes (Figure 4C, upper panel), whereas miR-30 sponge transfection alone was sufficient to increase its activity (Figure 4C, lower panel). Moreover, miR-30a overexpression significantly decreased PAN-induced nuclear translocation of NFATC3, and both FK506 and DEX exerted a similar effect (Figure 4D). miR-30a overexpression also reduced TGF- $\beta$ - or LPS-induced intracellular  $\text{Ca}^{2+}$  accumulation and

calcineurin phosphatase activity in the podocytes (Supplemental Figure 9, A and B). TGF- $\beta$  and LPS also upregulated calcineurin protein expression levels (Supplemental Figure 9C). Similar to PAN, TGF- $\beta$  and LPS are capable of downregulating miR-30s in podocytes, as we have previously demonstrated (9).

We also used another type of miR inhibitor, locked nucleic acid-modified (LNA-modified) 8-mer anti-miR, which targets the seed sequence of miRs, thereby inhibiting all members of a miR family (40). LNA-anti-miR-30s increased the protein levels of TRPC6, PPP3CA, PPP3CB, PPP3R1, and NFATC3 in podocytes in the absence or presence of PAN (Supplemental Figure 10, A and B). Accordingly, calcineurin phosphatase activity in the cells was elevated (Supplemental Figure 10C).

Angiotensin II (Ang II) is known to be injurious to podocytes and plays a pathogenic role in glomerular diseases. We found that Ang II downregulated all members of the miR-30 family (Supplemental Figure 11A); that Ang II upregulated TRPC6, PPP3CA, PPP3CB, PPP3R1, and NFATC3 protein levels, an effect that was attenuated by exogenous miR-30a transfection (Supplemental Figure 11, B and C); and that miR-30a overexpression prevented Ang II-induced calcium influx, NFATC3 nuclear accumulation, increased calcineurin activity, and decreased SYNPO expression in the podocytes (Supplemental Figure 11, D-G). These results further demonstrate the pathogenic significance of the miR-30/calcium/calcineurin pathway.

*miR-30s prevent calcineurin-induced SYNPO degradation, thereby preserving actin fibers in podocytes.* Calcium/calcineurin signaling can induce actin fiber damage via SYNPO dephosphorylation and degradation in podocytes (33). We speculated that miR-30s protect actin fibers and the cytoskeleton by preventing calcineurin activation and, consequently, SYNPO degradation. Indeed, we observed that miR-30 silencing using the miR-30 sponge caused actin fiber disruption and loss in cultured podocytes and that these effects were mitigated by FK506 (Figure 5, A and B). LNA-anti-miR-30s also induced actin fiber disruption, which was prevented by FK506 (Figure 5, C and D). These results

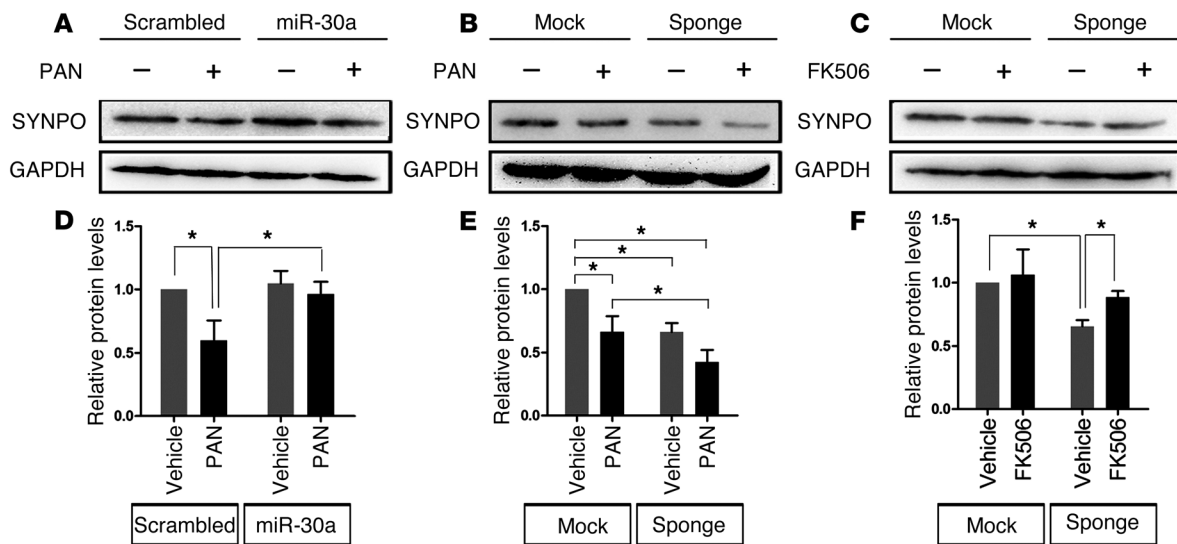


**Figure 6. miR-30s maintain SYNPO protein expression in podocytes.** (A) Immunoblotting showing that miR-30a overexpression prevented the PAN-induced loss of SYNPO expression. (B) The miR-30 sponge was sufficient to reduce SYNPO expression and augment the PAN-induced decrease in SYNPO expression. (C) FK506 prevented the effect of the miR-30 sponge on SYNPO expression. (D–F) Quantification of the results in A (D), B (E), and C (F). Parallel gels were run for SYNPO and GAPDH in each experiment. The results are expressed as the mean  $\pm$  SD of at least 3 experiments. Two-way ANOVA,  $*P < 0.05$ .

demonstrate that miR-30s maintain actin fiber structure and function by preventing increased calcineurin activity.

To examine the effect of miR-30s on SYNPO, we either overexpressed or silenced them using a sponge in podocytes in the presence or absence of PAN. We found that miR-30a overexpression prevented the PAN-induced loss of SYNPO expression (Figure 6, A and D), whereas miR-30 knockdown reduced its expression in both the absence and presence of PAN (Figure 6, B and E). As expected, miR-30 sponge-induced SYNPO loss was blocked by FK506 (Figure 6, C and F). These results suggest that the SYNPO degradation pathway is at least a component of the mechanism underlying PAN- or miR-30 sponge-induced actin fiber and cytoskeletal injury.

*The miR-30 sponge induces podocyte apoptosis, which is ameliorated by FK506.* We have previously shown that miR-30 loss induces apoptosis via Notch signaling (9). However, Notch signaling should not be the only mediator of miR-30 sponge-induced apoptosis, because the Notch inhibitor DBZ did not fully protect against apoptosis (Supplemental Figure 12). Because calcium/calcineurin signaling is known to induce podocyte apoptosis via the NFATC pathway (16, 17), we speculated that the miR-30 sponge also induces apoptosis via the calcium/calcineurin/NFATC signaling pathway. Indeed, we found that the proapoptotic effect of the miR-30 sponge was partially inhibited by FK506, as demonstrated by flow cytometric analysis of cells stained with annexin V (Figure 7, A and B). Calcineurin phosphatase activity was correlated with the apoptotic rates of the cells subjected to different treatments (Figure 7C). These results suggest that calcium/calcineurin/NFATC signaling is a component of the mechanism underlying miR-30 sponge-induced apoptosis.

*miR-30s prevent calcium-calcineurin-induced activation of integrin  $\beta$ 3.* Integrin  $\beta$ 3 (ITGB3) is known to be involved in podocyte injury (41), and it was shown to be an miR-30 target in cancer cells (42). We found that miR-30s do not affect ITGB3 protein expression in podocytes, because neither miR-30a nor miR-30

sponge overexpression altered its protein levels in podocytes (Figure 8A). However, miR-30a overexpression prevented its activation induced by PAN, as shown by staining with AP5 antibody that detects the active form of ITGB3 (Figure 8B). We also found that the calcineurin inhibitor FK506 and the NFATC inhibitor 11R-VIVIT prevented miR-30 sponge-induced ITGB3 activation, suggesting that miR-30s prevent ITGB3 activation through inhibition of the calcineurin/NFATC pathway. Interestingly, miR-30s can prevent protein upregulation of the urokinase plasminogen activator receptor (uPAR) (Figure 8C), which has been reported to enhance ITGB3 activity in podocytes (43).

*Transgenic miR-30 sponge induces proteinuria and podocyte foot process effacement, which are blocked by FK506 treatment and the delivery of miR-30a.* To demonstrate that miR-30s regulate calcium/calcineurin signaling in vivo, we constructed a conditional miR-30 sponge transgene (CAG-loxP-RFP-stop-loxP-EGFP-miR-30 sponge) (Figure 9A), in which the sponge fragment containing 11 miR-30 recognition sequences (Figure 9B) was inserted downstream of the EGFP coding region. The transgene expresses red fluorescent protein (RFP) but not EGFP or the miR-30 sponge because of the “stop” element preceding the EGFP and sponge sequence. We identified and used 2 independent transgenic lines (Figure 9C), which were indistinguishable in their phenotypes. RFP expression was observed on the skin (Figure 9D) and in glomeruli (Figure 9E). When crossed with a podocyte-specific *NPHS2-Cre* transgene, the double-transgenic mice ( $SP^+$ ) lost RFP expression in the glomeruli (Figure 9E), an indication of sponge expression. qPCR analysis detected sponge expression in the glomeruli of  $SP^+$  mice (Figure 9F).

The  $SP^+$  mice were viable and exhibited normal growth and body weight (data not shown). However, they developed significant proteinuria (Figure 10A) and podocyte foot process effacement (Figure 10B) 2–3 weeks after birth. The proteinuria persisted at a constant severity for at least 8 months, without the development

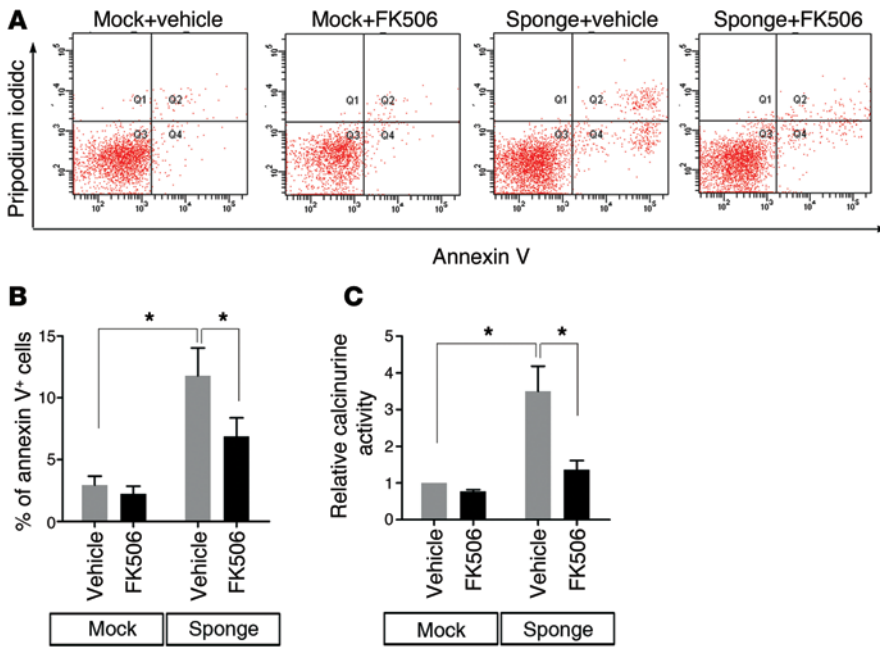


**Figure 7. miR-30 silencing using the miR-30 sponge induced podocyte apoptosis, which was prevented by FK506 treatment.** (A) Flow cytometric analysis of the annexin V-stained cells treated as indicated. (B) Normalized quantification of the results in A. (C) Calcineurin phosphatase activity assays of the cells treated as indicated. All experiments were repeated at least 3 times, and the results are expressed as the mean  $\pm$  SD. Two-way ANOVA, \* $P < 0.05$ .

of glomerulosclerosis. Analysis of isolated glomeruli from SP<sup>+</sup> mice revealed increases in both calcineurin phosphatase activity (Figure 10C) and proteins, accompanied by a decrease in SYNPO expression (Figure 10D), compared with control mice. Increased expression of TRPC6, PPP3CA, PPP3CB, PPP3R1, and NFATC3 proteins was clearly observed in the glomeruli of SP<sup>+</sup> mice by IHC analysis (Figure 10E). As expected, FK506 treatment reduced proteinuria and podocyte foot process effacement in these mice (Figure 10, F and G). Another calcineurin inhibitor, cyclosporine (CsA), also ameliorated the proteinuria in the transgenic mice (Figure 10H).

We further examined the mice to determine podocyte numbers and found an 11.8% reduction in these numbers compared with those in control mice ( $n = 8$ ;  $P < 0.05$ ) (Supplemental Figure 13A). In addition to the SYNPO downregulation shown in Figure 9D, additional podocyte differentiation markers, podocin and nephrin, were also reduced in the SP<sup>+</sup> mice (Supplemental Figure 13, B and C). TUNEL assays showed no apoptotic podocytes in the SP<sup>+</sup> mice (data not shown); however, glomerular expression levels of the proapoptotic markers BAX, FAS, and APAF1 were increased, whereas antiapoptotic BCL2 expression was reduced (Supplemental Figure 13D), suggesting a low level of podocyte apoptosis in the mice.

We treated SP<sup>+</sup> mice and their control littermates with a high dose of Adriamycin (ADR) (44). We found that the control mice exhibited mild proteinuria and podocyte loss but not glomerulosclerosis after ADR treatment (Supplemental Figure 14, A–C), demonstrating that they were resistant to ADR compared with BALB/c mice, which are routinely used for ADR-induced podocyte injury and glomerulosclerosis. In contrast, ADR-treated SP<sup>+</sup> mice had moderate levels of proteinuria and further loss of podocytes (Supplemental Figure 14, A and B), and, importantly, we clearly observed sclerotic glomeruli (Supplemental Figure 14C), although they were sporadic (~5%).

To confirm that the miR-30 sponge acts specifically via the loss of function of miR-30, we performed a rescue experiment in

which lentivirus-expressing miR-30a was injected into the kidneys of SP<sup>+</sup> mice. We found that exogenous miR-30a was successfully expressed in the glomeruli of the lentivirus-injected mice, as indicated by EGFP expression (Supplemental Figure 15A). Proteinuria (Supplemental Figure 15B) and foot process effacement (Supplemental Figure 15C) were significantly alleviated in these mice 3 days after lentivirus injection. These results clearly demonstrate the specificity of the miR-30 sponge.

*miR-30s repress calcium/calcineurin signaling in cardiomyocytes.* miR-30s are highly expressed and the fourth most abundant miRs in the heart (Supplemental Figure 16), according to the smiRNAdb database (<http://www.mirz.unibas.ch>). miR-30s are downregulated in response to injurious stimuli in cardiomyocytes (45). Because calcium/calcineurin signaling is known to be involved in cardiomyocyte injury and cardiac hypertrophy (24–28), we speculated that miR-30s may also regulate calcium/calcineurin signaling in cardiomyocytes.

To test this hypothesis, we transfected a rat cardiomyocyte cell line with the miR-30 sponge and found that PPP3CA, PPP3CB, and NFATC3 protein expression levels were markedly increased (Supplemental Figure 17), although no changes in the protein expression levels of TRPC6 or PPP3R1 were observed in these cells under these experimental conditions. As expected, increased calcineurin activity (Supplemental Figure 18A) and the nuclear translocation of NFATC3 (Supplemental Figure 18B) were observed in these cells. We performed phalloidin staining (Supplemental Figure 18C) and found that the miR-30 sponge increased the size of the transfected cells and that this effect was prevented by FK506 (Supplemental Figure 18D), suggesting that the miR-30 sponge induced cardiomyocyte hypertrophy. In support of this finding, qPCR analysis of hypertrophy markers showed that the expression levels of *Myl7* and *Nppa* were increased, whereas *Myl6* levels were decreased in the cells transfected with the miR-30 sponge (Supplemental Figure 18E). We also observed that miR-30 sponge transfection resulted in increased apoptosis, which was attenuated by FK506 (Supplemental Figure 18F).

## Discussion

Our previous studies have demonstrated an association between miR-30 deficiency and actin fiber instability in podocytes, potentially via calcium/calcineurin signaling (9). This observation motivated us to explore the relationship between miR-30s and calcium/calcineurin signaling. In support of this, bioinformatics

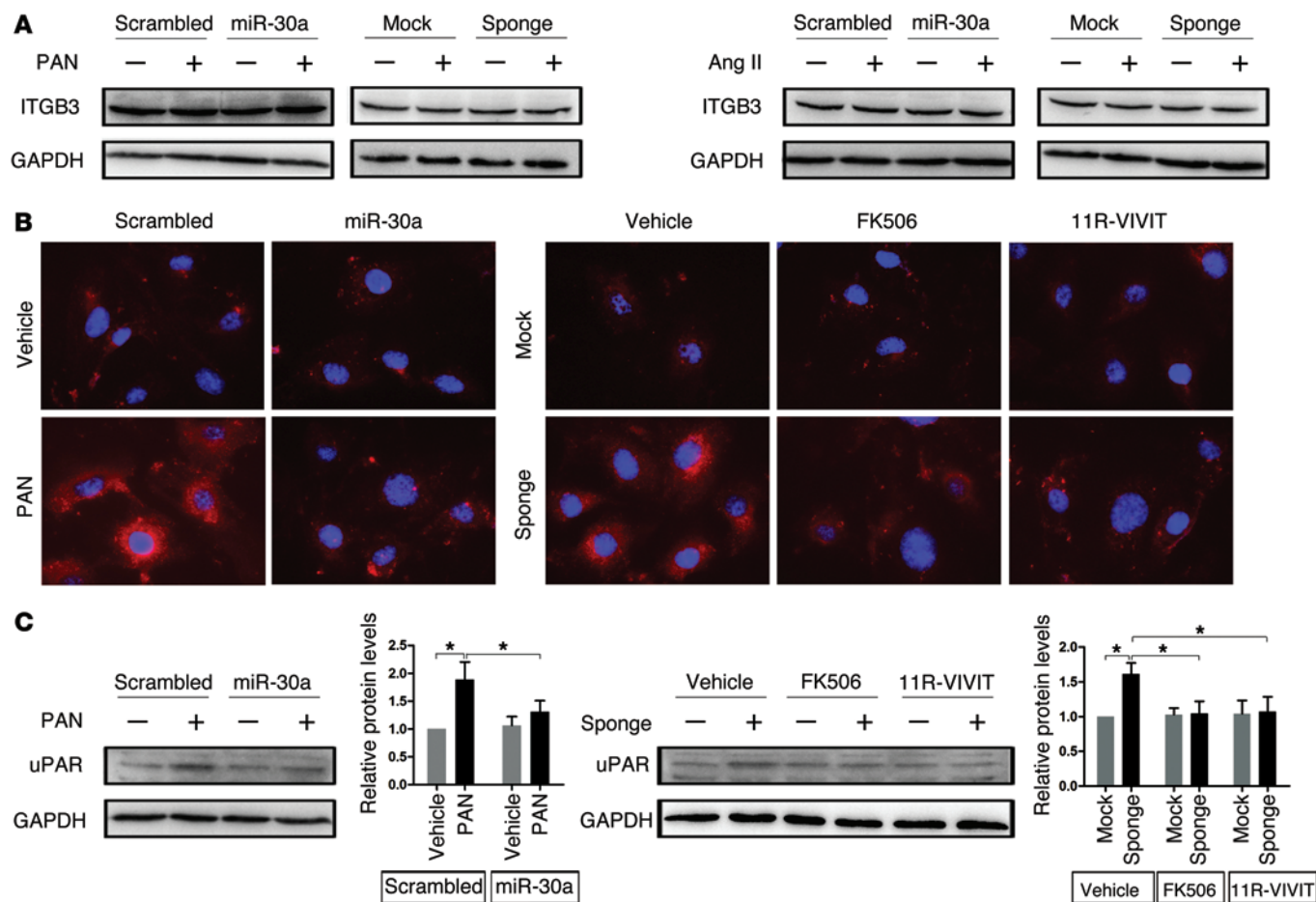


**Figure 8. miR-30s do not inhibit ITGB3 protein expression but suppress its activity.** (A) Neither exogenous miR-30a nor sponge transfection changed the protein levels of ITGB3 in cultured podocytes in the absence or presence of PAN or Ang II. (B) AP5 assays showed that ITGB3 activity was enhanced by PAN or by the miR-30 sponge, but the enhancement could be blocked with miR-30a, FK506, or 11R-VIVIT. Original magnification,  $\times 20$ . Representative images from 3 independent experiments are shown. (C) Representative immunoblots showing that uPAR could be upregulated by PAN or the miR-30 sponge, but the upregulation could be blocked by exogenous miR-30a, FK506, or 11R-VIVIT. Parallel gels were run for ITGB3 or uPAR and the loading control (GAPDH) in all immunoblotting experiments. Quantification was performed on the basis of 3 independent experiments. Two-way ANOVA,  $*P < 0.05$ .

analysis of predicted miR-30 targets revealed the enrichment of genes associated with the calcium/calceinurin signaling pathway (Supplemental Table 1), including several critical components of this pathway, such as *TRPC6*, *PPP3CA*, *PPP3CB*, *PPP3R1*, and *NFATC3* (Supplemental Table 2). We hypothesized and ultimately demonstrated that miR-30s inhibit calcium/calceinurin signaling by targeting these critical factors.

*TRPC6*, *PPP3CA*, *PPP3CB*, *PPP3R1*, and *NFATC3* belong to the 4 gene families TRPC, PPP3C, PPP3R, and NFATC, respectively. Surprisingly, we found that the miR-30-targeted factors *TRPC6*, *PPP3CA*, *PPP3CB*, *PPP3R1*, and *NFATC3* were expressed at high mRNA levels, whereas the non-miR-30-targeted family members (except for *TRPC1*) were expressed at low mRNA levels in podocytes, suggesting that they play major roles in calcium/calceinurin signaling in these cells. The findings that miR-30s selectively target these 5 most important genes and that these 5 genes function at multiple critical steps of the calcium/calceinurin signaling pathway support our hypothesis that miR-30s tightly regulate calcium/calceinurin signaling in podocytes. Importantly, the dominant expression of *TRPC6*, *PPP3CA*, *PPP3CB*, *PPP3R1*, and

*NFATC3* relative to expression of other family members in podocytes was recapitulated in humans, as demonstrated by microarray gene expression profiling of normal human glomeruli (Supplemental Figure 2, A and B).

In contrast to the high mRNA levels of these factors, the proteins encoded by these 5 genes were barely detected in normal podocytes of both rodents and humans, suggesting the posttranscriptional regulation of their expression. However, the expression of these proteins was markedly increased in the podocytes of PAN-treated rats, FSGS patients, and SP<sup>+</sup> mice (Supplemental Figure 3, Figure 2, and Figure 9) in the absence of significant mRNA upregulation (except for *TRPC6*) (Figure 2 and Supplemental Figure 4). These results demonstrated that miR-30s inhibit the expression of these genes at the translational level and that loss of function of miR-30s leads to the upregulation of these proteins. Upregulation of *Trpc6* mRNA expression in the podocytes of the PAN-treated rats, but not in those of patients with FSGS, is consistent with the previous finding of positive feedback between calcineurin/NFATC signaling and *TRPC6* gene transcription (46). Thus, the upregulation of *TRPC6* protein expression in injured podocytes may occur

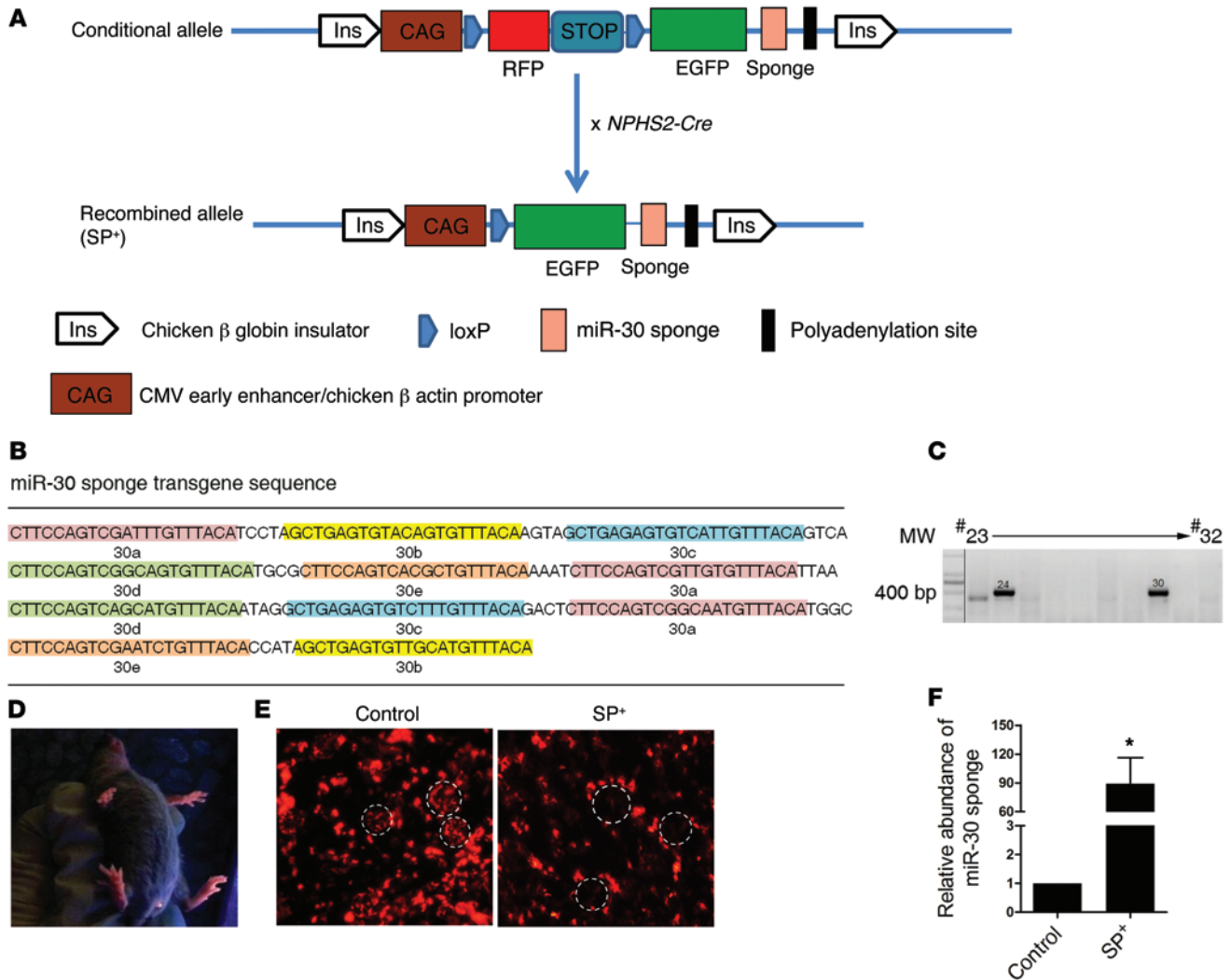


**Figure 9. The generation of miR-30 sponge transgenic mice.** (A) Schematic of the structure of the conditional miR-30 sponge transgene and the resulting product of recombination induced by Cre. (B) Sequence of the miR-30 sponge transgene. The 11 miR-30 cognate sequences are indicated. (C) Identification by PCR of the founders carrying the transgene. The “MW” lane, which was originally on the right, has been moved to the left. (D) Red fluorescence of the body of a transgenic mouse. (E) Crossing the conditional miR-30 sponge transgenic mice with *NPHS2-Cre* transgenic mice resulted in the loss of RFP expression in podocytes, presumably resulting in expression of the miR-30 sponge. Original magnification,  $\times 40$ . The failure to observe EGFP expression may be due to the following 2 reasons: 1) the miR-30 sponge sequence at the 3’UTR of EGFP may have recruited the miR-30-guided Ago complex that inhibits EGFP translation; and 2) the *CAG* promoter may have been inhibited in the injured podocytes (66). RFP appeared to be expressed only in podocytes but not in other cell types in the glomeruli. A similar phenomenon has been observed for a transgene carrying a ubiquitous *CMV* promoter (7). (F) qPCR analysis of sponge expression in the glomeruli from conditional miR-30 sponge transgenic mice ( $n = 3$ ) and double-transgenic mice (SP<sup>+</sup>) ( $n = 3$ ) demonstrated the successful induction of miR-30 sponge expression in the glomeruli of SP<sup>+</sup> mice. Two-tailed Student’s *t* test,  $*P < 0.05$ .

via 2 distinct mechanisms, translational de-repression via miR-30 downregulation and transcriptional upregulation via TRPC6-promoted calcineurin/NFATC signaling. It will be important to determine the relative contributions of these 2 mechanisms to TRPC6 protein upregulation and to understand why the positive feedback between calcineurin/NFATC signaling and *TRPC6* mRNA expression does not occur in the podocytes of patients with FSGS.

In addition to TRPC6, TRPC1 is highly expressed in both rodent and human podocytes/glomeruli (Figure 1 and Supplemental Figure 2). The role of TRPC1 in podocyte injury has been elusive. It is known that *Trpc1*-KO mice lack renal lesions (47). Both glucose and H<sub>2</sub>O<sub>2</sub> upregulate TRPC6, but not TRPC1, in podocytes (48, 49). We also found that mRNA expression of *TRPC6*,

but not *TRPC1*, was upregulated in the podocytes of experimental animal models and in those of patients with FSGS. Moreover, whether TRPC1 functions as an independent ion channel (similar to TRPC6) or simply as a regulatory unit that binds to other TRPC family members to facilitate their functions remains under debate (50). On the basis of these studies, we speculate that TRPC1 may not serve as a critical factor for calcium/calcineurin signaling activation in podocytes.

Our functional studies clearly demonstrated that miR-30s regulate calcium/calcineurin signaling and that the loss of this regulation results in podocyte injury. In vitro, miR-30 silencing using the miR-30 sponge increased the expression of TRPC6, PPP3CA, PPP3CB, PPP3R1, and NFATC3, proteins, Ca<sup>2+</sup> influx,

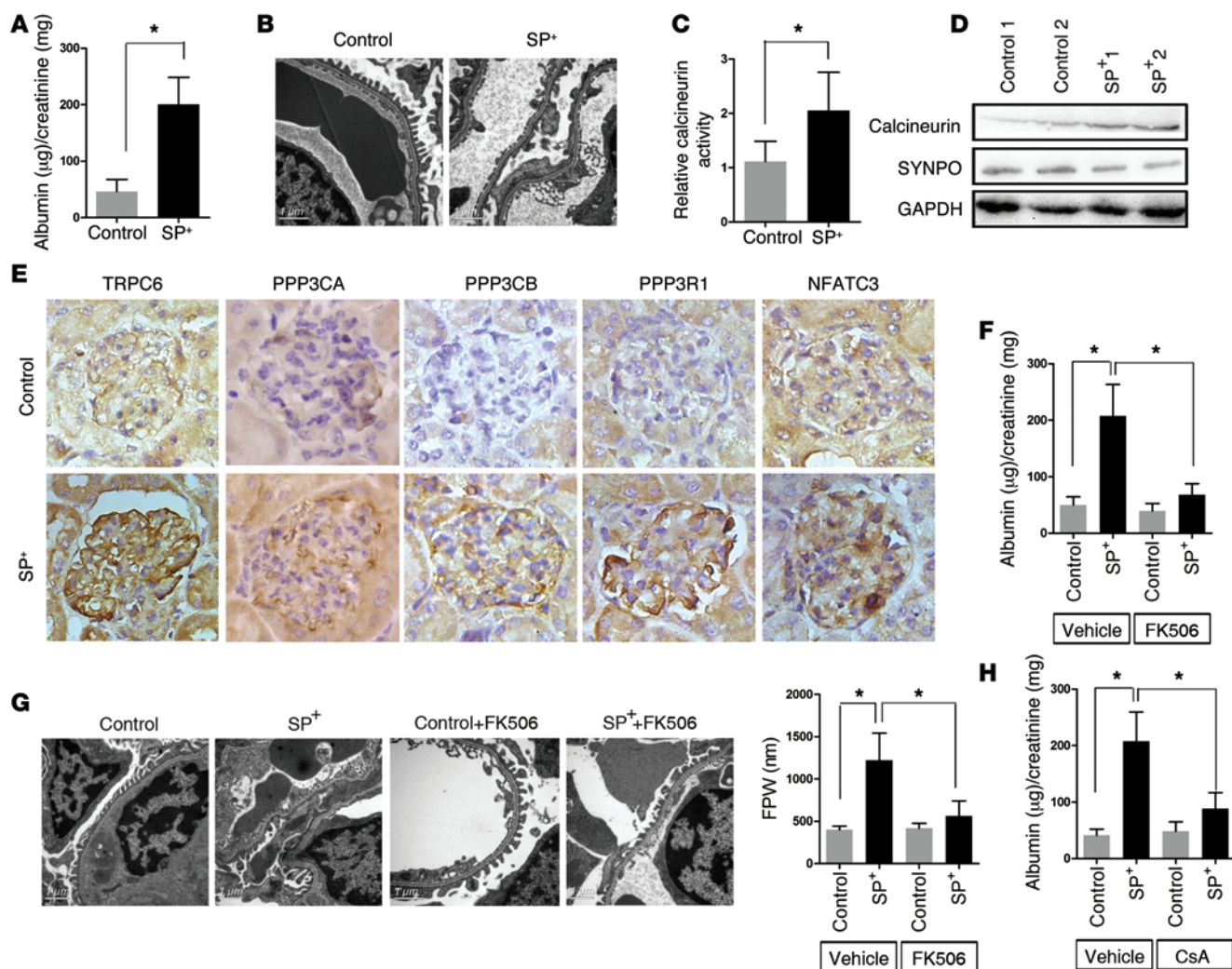


**Figure 10. Characterization of the miR-30 sponge-expressing transgenic (SP<sup>+</sup>) mice.** (A) The SP<sup>+</sup> mice developed significant proteinuria ( $n = 10$ ). Two-tailed Student's  $t$  test,  $*P < 0.05$ . (B) Electron microscopic examination of the kidneys of SP<sup>+</sup> mice revealed massive foot process effacement of the podocytes. Representative images from 6 mice in each group are shown. Scale bars: 1  $\mu\text{m}$ . (C) The calcineurin phosphatase assay of the isolated glomeruli demonstrated increased calcineurin activity in the glomeruli of SP<sup>+</sup> mice compared with that in control mice ( $n = 5$  each). Two-tailed Student's  $t$  test,  $*P < 0.05$ . (D) Immunoblotting of the isolated glomeruli revealed increased expression of calcineurin and decreased expression of SYNPO in the glomeruli of SP<sup>+</sup> mice. Parallel gels were run for calcineurin or SYNPO and GAPDH. (E) IHC showing that TRPC6, PPP3CA, PPP3CB, PPP3R1, and NFATC3 protein expression levels were upregulated in the glomeruli of SP<sup>+</sup> mice. Original magnification,  $\times 40$ . Representative images from 6 mice in each group are shown. (F) FK506 reduced proteinuria in SP<sup>+</sup> mice ( $n = 8$ ). Two-way ANOVA,  $*P < 0.05$ . (G) Electron microscopic image showing that FK506 abolished podocyte foot process effacement in SP<sup>+</sup> mice ( $n = 4$ ). Quantification of the results is shown on the right. FPW, foot processes width. Scale bars: 1  $\mu\text{m}$ . Two-way ANOVA,  $*P < 0.05$ . (H) CsA treatment of SP<sup>+</sup> mice significantly reduced proteinuria ( $n = 8$ ). Two-way ANOVA,  $*P < 0.05$ .

the Ca<sup>2+</sup> intracellular concentration, calcineurin activity, and the nuclear translocation of NFATC3 in cultured podocytes. In addition, this sponge induced cytoskeletal injury and apoptosis in the cells, both of which were prevented by FK506 treatment. In vivo, we generated transgenic mice in which miR-30 expression was silenced in podocytes and observed proteinuria, podocyte foot process effacement, and increased expression of TRPC6, PPP3CA, PPP3CB, PPP3R1, and NFATC3 proteins in these cells. Both proteinuria and foot process effacement were reversed by exogenous miR-30 delivery, clearly demonstrating the role of miR-30s in podocyte homeostasis. The abolishment of these phenotypes via FK506 treatment clearly indicated that calcium/calcineurin signaling mediates the effect of miR-30 silencing in

podocytes. In contrast, glucocorticoid treatment did not ameliorate the effect of the miR-30 sponge on podocytes, because glucocorticoids only prevent TGF- $\beta$ - or PAN-induced miR-30 downregulation at the transcriptional level and do not increase miR-30 expression (9). Therefore, glucocorticoids exert no effects on miR-30s in cells containing a miR-30 sponge.

Recently, ITGB3 was reported to be a miR-30 target in cancer cells (42). It is also known that ITGB3 is involved in podocyte injury (41), raising the possibility that direct inhibition of ITGB3 by miR-30s may contribute to the protective effect of miR-30s on podocytes. We investigated this question and found that miR-30s did not inhibit ITGB3 protein expression in podocytes (Figure 8A). However, miR-30s did inhibit ITGB3 activity (Figure 8B). Because uPAR

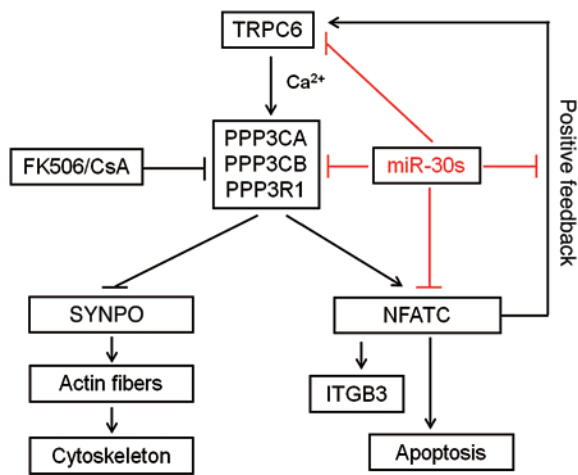


**Figure 11. Working model of the relationship between miR-30s, calcium/calcineurin signaling, and actin stability in podocytes.**

is known to enhance ITGB3 activity and function (43) and its expression is driven directly by NFATC transcriptionally (43), miR-30s should be capable of inhibiting uPAR expression. Indeed, we found that miR-30a overexpression downregulated uPAR, while the miR-30 sponge upregulated uPAR (Figure 8C), suggesting that miR-30s inhibit ITGB3 function in podocytes by blocking the calcineurin/NFATC/uPAR pathway, but not through direct targeting. The contribution of increased ITGB3 activity to the podocyte injury induced by miR-30 deficiency warrants further investigation.

Why do miR-30 sponge transgenic mice (SP<sup>+</sup>) lack glomerulosclerosis? Since podocyte depletion is considered to underlie glomerulosclerosis (1, 51), we speculate that the functional loss of miR-30s in SP<sup>+</sup> mice was not sufficient for adequate podocyte apoptosis (or detachment) and thus depletion. To prove this, we quantified sponge copy numbers in the podocytes of SP<sup>+</sup> mice as well as in the sponge-transfected cultured podocytes, which undergo robust apoptosis (9). We found that the copy numbers of miR-30 in mouse podocytes *in vivo* and in cultured podocytes were comparable (Supplemental Figure 19A); however, we found much lower sponge copy numbers in the former compared with the latter (Supplemental Figure 19B). The ratio of sponge/miR-30s in the former was also much lower (~4.4-fold) than that in the latter (Supplemental Figure 19C), suggesting differential miR-30 functional losses in the 2 cases. As expected, miR-30 levels in both SP<sup>+</sup> mice podocytes and sponge-transfected cultured podocytes had only moderate reductions compared with controls (Supplemental Figure 19, D and E), indicating that the sponge acts as a miR decoy to bind the miR but does not degrade it efficiently (52). Consistent with the above results, we did not detect apoptotic podocytes by TUNEL assay in the SP<sup>+</sup> mice, which is in contrast with the robust apoptosis observed in the sponge-transfected cultured podocytes. However, a low level of apoptosis might have been present in the podocytes of the SP<sup>+</sup> mice, as suggested by the 11.8% loss of podocytes in these mice (Supplemental Figure 13A), the moderately increased expression of the apoptotic markers BAX, FAS, and APAF1, and the decreased expression of antiapoptotic BCL2 (Supplemental Figure 13D). This level of podocyte loss in the SP<sup>+</sup> mice is certainly not sufficient to

cause the development of glomerulosclerosis, according to a study in which various degrees of podocyte depletion were evaluated to determine the relationship between podocyte loss and glomerulosclerosis (53). This study showed that a podocyte loss of less than 20% did not result in glomerulosclerosis, 21% to 40% led to focal segmental glomerulosclerosis, and a greater than 40% loss resulted in segmental to global glomerulosclerosis. The findings of another study in diabetic mice were consistent with this result (47). Together, these results support our speculation that the lack of glomerulosclerosis in the SP<sup>+</sup> mice was most likely due to the insufficient loss of podocyte apoptosis and depletion. This speculation is further supported by the fact that the SP<sup>+</sup> mice had a significantly increased sensitivity to ADR treatment, resulting in moderate proteinuria and low levels of glomerulosclerosis (Supplemental Figure 14). Apparently, a combined of knockout of all 6 miR-30 genes (miR-30c is encoded by 2 separate genes) is needed for a definitive conclusion.

Nevertheless, the contribution of miR-30-mediated TRPC6/calcineurin signaling to human FSGS requires further investigation. First, the actions of TRPC6/calcineurin signaling in podocytes are complicated and even controversial. Although TRPC6/calcineurin activation was shown to induce podocyte injury (31, 32), a recent study showed that TRPC6/calcineurin activation did not cause immediate podocyte injury and could even protect podocytes in the glomerular disease model of nephrotoxic serum (NTS) nephritis (32). Second, consistent with the previous study (54), we found that *TRPC6* mRNA was not significantly increased in the glomeruli of FSGS patients, unlike in the PAN-treated rats (Supplemental Figure 4), in which we have shown a critical role for miR-30s and their associated calcineurin signaling. This indicates a mechanistic difference in podocyte injury between human FSGS and PAN-induced glomerular injury in rats. Third, we observed that exogenous miR-30a overexpression did not fully rescue podocytes from injury, suggesting additional mechanisms underlying the injury. Last, since human FSGS is known to be heterogeneous in its pathogenesis, the involvement of miR-30s and the associated TRPC6/calcineurin signaling in different types of FSGS may be distinct.

On the basis of these studies, we have generated a working model illustrating the roles of miR-30s in podocyte homeostasis and injury and the relationship between miR-30s and other mediators of podocyte injury (Figure 11). This model also explains observations from previous studies. For example, it has been shown that LPS induces podocyte injury by activating calcineurin but that CsA protects podocytes by inhibiting calcineurin activity, thereby preventing the dephosphorylation and degradation of SYNPO (33). Now our model indicates that the ability of LPS to induce calcineurin activity is dependent on the downregulation of miR-30s. Indeed, we observed that miR-30s prevent PAN-induced SYNPO degradation (Figure 6). In summary, miR-30s may play an important role in podocyte homeostasis and pathogenesis and mediate the protective effect of glucocorticoids or FK506 and CsA on podocytes.

The findings in the present study may have broader significance. In a database search, we found that miR-30s are highly expressed in the heart (Supplemental Figure 16). Because previous studies have shown that miR-30s are downregulated in cardiomyocytes in response to damaging stimuli, e.g., ROS (45), and

that calcium/calcineurin signaling plays a critical role in cardiomyocyte injury and cardiac hypertrophy (25–28), we hypothesized that miR-30s also regulate calcium/calcineurin signaling in cardiomyocytes. We confirmed this hypothesis via miR-30 silencing by delivering a miR-30 sponge to cardiomyocytes (Supplemental Figure 18). Further studies should be performed to elucidate the role of miR-30s in the pathogenesis of cardiac diseases. Interestingly, according to IPA analysis, the predicted miR-30 targets are enriched in components of cardiac hypertrophic signaling, including TRPC6, PPP3CA, PPP3CB, PPP3R1, and NFATC3 (Supplemental Table 1). Apparently, cardiac hypertrophic signaling overlaps with calcium/calcineurin signaling as a result of the similarity between their components. In addition to cardiomyocytes, miR-30s may regulate calcium/calcineurin signaling in neurons. As shown in Supplemental Table 1, the predicted miR-30 targets are enriched in components of axon guidance signaling, including TRPC6, PPP3CA, PPP3CB, PPP3R1, and NFATC3. Database searches have revealed that miR-30s are highly expressed in neural tissues (data not shown). In fact, they have been shown to be regulated in neurons and involved in the pathogenesis of certain neural diseases (55, 56). It will be important to investigate whether the tight regulation of calcium/calcineurin signaling by miR-30s also occurs in neurons to modulate neuronal synaptic transmission, a cellular process that involves calcium signaling (57).

In conclusion, our study demonstrated that miR-30s control calcium/calcineurin signaling by directly inhibiting TRPC6, PPP3CA, PPP3CB, PPP3R1, and NFATC3 in podocytes and cardiomyocytes. The downregulation of miR-30s results in the activation of calcium/calcineurin signaling, leading to injuries to podocytes and other cell types. Our findings may provide novel insights into the pathogenesis of injuries to podocytes and cardiomyocytes and suggest that the targeting of miR-30s may represent an effective therapeutic approach to treat podocytopathy and other diseases.

## Methods

**Human kidney samples.** All FSGS cases were diagnosed on the basis of renal biopsies performed at the National Clinical Research Center of Kidney Diseases of the Nanjing University School of Medicine. Kidney biopsies from patients with FSGS and normal kidney tissues from nephrectomy patients were obtained from this center's renal biorepository.

**Human renal tissue handling and microdissection to collect glomeruli.** Renal biopsies were immediately fixed in formalin and embedded in paraffin according to standard procedures. Alternatively, renal biopsies were embedded in OCT compound and immediately frozen. For glomeruli collection, the patients' renal biopsies were placed in RNAlater (Ambion) and stored at  $-70^{\circ}\text{C}$ . Microdissection to collect glomeruli was manually performed under a stereomicroscope using 2 dissection needle holders in RNAlater at  $4^{\circ}\text{C}$ . For the calcineurin activity assay, freshly collected biopsies were placed in lysis buffer containing protease inhibitors and homogenized on ice to extract soluble proteins for use in the assay.

**Animals.** Transgenic mice specifically expressing a miR-30 sponge in podocytes were generated by the Model Animal Research Center at Nanjing University. Briefly, a DNA fragment encoding a miR-30 sponge that contained 11 miR-30 cognate sites in total (Figure 9B) was synthesized and inserted downstream of the EGFP coding region of

the vector pCAG-loxP-RFP-stop-loxP-eGFP (Model Animal Research Center of Nanjing University), resulting in the transgenic construct shown in Figure 9A. Pronuclear injection was performed with this construct following standard protocol, and the resulting progenies were subject to PCR genotyping using the primers located as indicated in Figure 9A (forward primer: 5'-TACAGCTCCTGGGCAACGTGC; reverse primer: 5'-CACGTACACCTTGGAGCCGTAC). Two independent founders were used for the generation of the mice with podocyte-specific miR-30 sponge expression via *NPHS2-Cre* (35).

To isolate podocytes from mice for various experiments, transgenic mice, in which the podocytes were labeled with EGFP, were generated by crossing Gt(ROSA)26Sor<sup>tm4(ACTB-tdTomato, eGFP)</sup>Luo (34) transgenic mice with *NPHS2-Cre* transgenic mice (35), and the double-transgenic mice were used for podocyte isolation via FACS (MoFlo XDP; Beckman Coulter) (Supplemental Figure 1) following the method described previously (58).

**Urinary albumin and creatinine measurements.** Urinary albumin and creatinine levels in the mice were measured using Albuwell M and Creatinine Companion Kits (Exocell Inc.) according to the manufacturer's instructions.

**Treatment of miR-30 sponge transgenic mice with calcineurin inhibitors.** FK506 (Fujisawa Pharmaceutical, Astellas Pharma Inc.) was dissolved in ethanol and sterile saline at a concentration of 0.5 mg/ml and was injected i.p. once per day into each mouse at a dose of 3 mg/kg. The vehicle solution contained the same concentrations as those of the solvents. Spot urine samples were collected in the morning. CsA (Calbiochem) (20 mg/kg/day) was similarly injected into mice.

**ADR treatment of mice.** Mice (control and SP<sup>+</sup> mice, 10 weeks of age) were treated with ADR (Sigma-Aldrich) at a dose of 18 mg/kg via tail-vein injection (44). Urine samples were collected for proteinuria assessment. The mice were sacrificed for pathological analyses 3 weeks after ADR injection.

**miR-30a-expressing lentivirus preparation and intrarenal injection.** A lentivirus expressing EGFP and miR-30a was purchased from HanBio (www.hanbio.net). We directly injected the virus into the mouse kidney according to previously described methods (59, 60). Briefly, we anesthetized the mice and occluded the left renal pedicle. Then, we inserted a 31-gauge needle on a syringe from the lower pole of the left kidney to the upper pole along the long axis of the kidney. The needle was slowly withdrawn, while 100  $\mu\text{l}$  lentivirus ( $\sim 1 \times 10^5$  IU/ $\mu\text{l}$ ) expressing EGFP alone (control) or EGFP and miR-30a was continuously released. The occlusion of the renal pedicle was reversed after the injection.

**Quantification of podocyte foot process effacement.** We quantified the foot process effacement of the podocytes using a previously described method (61, 62).

**Counting of mouse podocyte numbers.** We used a previously described method (63) to count podocytes in the glomeruli of control and SP<sup>+</sup> mice.

**Human podocyte culture and treatments.** The human podocyte cell line was provided by M. Saleem (University of Bristol, Bristol, United Kingdom), and the cells were cultured as previously described (64). The podocytes were treated with 5 ng/ml TGF- $\beta$  (R&D Systems); 50  $\mu\text{g}/\text{ml}$  PAN (Sigma-Aldrich); 10  $\mu\text{g}/\text{ml}$  LPS (Sigma-Aldrich); 1  $\mu\text{M}$  DEX (Sigma-Aldrich);  $10^{-6}$  mol/l Ang II (Sigma-Aldrich); and/or 1  $\mu\text{M}$  FK506. For transient transfection of plasmid DNA, FuGENE 6 Reagent (Roche Applied Science) was used according to the manufacturer's instructions. Transfection of LNA-anti-miR-30s (5'-TGTTTACAmU-3') and scram-

bled sequence (5'-TCATACTAmU-3') were performed with FuGENE 6 Reagent according to the manufacturer's instructions. To generate podocytes stably expressing miR-30a, the cells were transfected with the miR-30a expression construct, followed by selection using hygromycin.

*Preparation of a miR-30-expressing construct and a miR-30 sponge.* Preparation of the miR-30-expressing construct and the miR-30 sponge was performed as described in our previous report (9).

*Calcineurin phosphatase activity assay.* Calcineurin activity in the renal cortex and cultured podocytes was analyzed using a Biomol Calcineurin Cellular Activity Assay Kit according to the manufacturer's instructions. Briefly, freshly collected biopsies or cultured cells were placed in lysis buffer containing protease inhibitors and were homogenized on ice to extract soluble proteins. The free phosphate in the protein samples was removed by passing the samples through freshly prepared columns containing desalting resin. To measure calcineurin phosphatase activity, the protein sample concentrations were determined, and equal protein amounts were incubated in the substrate for 30 minutes. Liberated phosphate was measured colorimetrically at 620 nm. Calcineurin activity was calculated using a simultaneously prepared standard curve.

*Measurement of Ca<sup>2+</sup> influx and the intracellular Ca<sup>2+</sup> concentration.* Briefly, podocytes transfected with a mock control, a miR-30a-expressing construct, or a miR-30 sponge were treated with 50 µg/ml PAN for 24 hours. Then, the cells were incubated in the Ca<sup>2+</sup> indicator Fluo-3 (Thermo Fisher Scientific) in Ca<sup>2+</sup>-free buffer for 45 minutes. Receptor-operated channels were activated via the addition of 100 µM 1-oleoyl-2-acetyl-sn-glycerol (OAG). Then, 2 mM Ca<sup>2+</sup> was added to the cells to detect the changes in Ca<sup>2+</sup> levels mediated by the membrane-associated Ca<sup>2+</sup> channels. Images were captured every 5 seconds using a Zeiss LSM710 confocal microscope.

The cytosolic Ca<sup>2+</sup> concentration was assessed using the Ca<sup>2+</sup> indicator Fluo-3-AM. Podocytes were collected via trypsinization, followed by centrifugation at 200 g for 5 minutes. Then, the cells were washed with PBS, incubated in 5 mM Fluo-3/AM dye for 45 minutes at 37°C, and subjected to FACSscan flow cytometric analysis (BD). The Ca<sup>2+</sup> concentration was calculated according to Grynkiewicz et al. (65). In the end, the cells were incubated with 5 µM ionomycin in a zero Ca<sup>2+</sup> bath (0 Ca<sup>2+</sup>, 5 mM EGTA) and 5 µM ionomycin in saturating Ca<sup>2+</sup> solution (5 mM Ca<sup>2+</sup>), respectively, for the measurement of minimal and maximal responses to Ca<sup>2+</sup>.

*IHC and IF.* We prepared 5-µm sections of the paraffin-embedded kidneys and subjected these sections to IHC using peroxidase-conjugated antibodies and DAB for visualization. For IF staining, 5-µm sections of frozen tissue samples were blocked with BSA and incubated in primary antibodies against TRPC6 (catalog ab63038; Abcam); calcineurin (catalog 07-1490; EMD Millipore); PPP3CA (catalog sc-56953; Santa Cruz Biotechnology Inc.); PPP3CB (catalog 55148-1-AP; Proteintech); PPP3R1 (catalog ab115268; Abcam); NFATC3 (catalog sc-8405; Santa Cruz Biotechnology Inc.); SYNPO (catalog sc-21537; Santa Cruz Biotechnology Inc.); and ITGB3 (AP5) (catalog P05106; Karafast). Then, the sections were incubated with an FITC-conjugated anti-goat secondary antibody (Dako) or a Cy3-conjugated anti-rabbit/anti-mouse antibody (Dako), and the sections were mounted using Fluoromount (Sigma-Aldrich). The slides were examined using a Zeiss LSM710 confocal microscope or a Leica microscope (DM5000B).

*miR-30 target and function prediction.* The predicted miR-30 targets were obtained from TargetScan. IPA was used to predict the miR-30s functions.

*RNA extraction and qPCR analysis.* Cultured podocytes were subjected to small RNA or total RNA extraction after treatment using a mirVana miRNA Extraction Kit (Ambion). The RNA samples were used for miR quantification via qPCR with a kit purchased from Takara Biotechnology. The qPCR primers and sequences used are described in Supplemental Table 4.

*Determination of copy numbers of miR-30s and sponge in podocytes.* To determine copy numbers of miR-30s and sponge in podocytes, we performed qPCR for absolute quantification. A synthetic miR with a known concentration was purchased from Takara Biotechnology and was diluted serially (10<sup>1</sup>, 10<sup>2</sup>, 10<sup>3</sup>, 10<sup>4</sup>, and 10<sup>5</sup> fmol/l), followed by reverse transcription and qPCR. The resulting cycle threshold (Ct) values were plotted against the concentrations to make a standard curve. The absolute concentration of miR-30s was calculated on the basis of the equation generated by the standard curve and was transformed into copy numbers per microliter. To determine sponge copy numbers, we used the sponge expression plasmid for standard curve construction. The plasmid DNA was diluted serially at concentrations of 10<sup>3</sup>, 10<sup>4</sup>, 10<sup>5</sup>, 10<sup>6</sup>, 10<sup>7</sup>, 10<sup>8</sup>, and 10<sup>9</sup> copies/µl, respectively, and subjected to qPCR analysis. The standard curve was made by plotting the Ct values against the concentrations of the samples (copy numbers/µl) and was used to calculate the sponge concentrations in the samples tested. To calculate the copy numbers of miR-30s or sponge per mouse podocyte, the total numbers of mouse podocytes used for the calculation were estimated on the basis of the results shown in Supplemental Figure 13A.

*Quantification of the actin cytoskeleton.* Rhodamine-labeled phalloidin was used to stain F-actin in the podocytes, and the resulting images were obtained by confocal microscopy and digitized. The rhodamine-stained areas of the actin fibers were converted to black pixels and then inverted, followed by quantification using ImageJ software (NIH). The grayscale values ranged from 0 (black) to 200 (white, the maximal actin content). The mean podocyte actin content per pixel and the total actin content per cell were calculated and expressed as AU.

*Rat cardiomyocyte culture and treatments.* Rat embryonic heart-derived H9c2 cells were obtained from American Type Culture Collection (ATCC). The cells were cultured in DMEM (Gibco) supplemented with 10% FBS (Gibco) in an atmosphere of 5% (v/v) CO<sub>2</sub> and 95% air at 37°C. Transient transfection was performed using Lipofectamine 2000 (Invitrogen) according to the manufacturer's instructions.

*Cardiomyocyte IHC and cell-surface area analysis.* After treatment, the cultured cardiomyocytes were fixed in 4% paraformaldehyde for 15 minutes and permeabilized using 0.1% Triton X-100 in PBS, followed by blocking with 5% goat serum in PBS for 1 hour at room temperature. Then, the cells were stained for F-actin (rhodamine-labeled phalloidin). Cell nuclei were stained with DAPI. Images were captured using a Leica microscope (DM5000B). Cell-surface areas were calculated using ImageJ software.

*Luciferase reporter assay.* The 3'-UTRs of TRPC6, PPP3CA, PPP3CB, PPP3R1, and NFATC3 mRNAs were obtained via PCR using human genomic DNA as the template. These 3'-UTRs were inserted downstream of the pGL3 promoter (Promega). Site-directed mutagenesis was conducted to generate mutations in the region corresponding to the miR-30 "seed." The resulting constructs were cotransfected with Renilla-luciferase into podocytes using FuGENE 6 Reagent. Twenty-four hours later, cell lysates were prepared and subjected to luciferase assays using a Dual-Luciferase Reporter Assay System (Promega). Firefly luciferase activity was normalized to the corresponding Renilla-luciferase activity.

**Western blot analysis.** Cell lysates were prepared using radioimmunoprecipitation assay (RIPA) buffer containing a protease inhibitor cocktail (Roche) and a phosphatase inhibitor. The membranes were incubated with primary antibodies against TRPC6 (catalog ab63038; Abcam); calcineurin (catalog 07-1490; EMD Millipore); PPP3CA (catalog 07-067; EMD Millipore); PPP3CB (catalog ab96573; Abcam); PPP3R1 (catalog ab115268; Abcam); NFATC3 (catalog sc-8405; Santa Cruz Biotechnology Inc.); SYNPO (catalog sc-21537; Santa Cruz Biotechnology Inc.); nephrin (catalog ab58968; Abcam); podocin (catalog ab50339; Abcam); uPAR (catalog sc-10815; Santa Cruz Biotechnology Inc.); and ITGB3 (catalog sc-14009; Santa Cruz Biotechnology Inc.).

**Flow cytometric analysis of apoptosis via annexin V staining.** After treatment, the podocytes were collected, washed twice with ice-cold PBS, resuspended in 200  $\mu$ l binding buffer, and then incubated in FITC-conjugated annexin V at a final concentration of 0.5  $\mu$ g/ml at room temperature for 15 minutes. Then, the cells were washed, centrifuged, and resuspended in 500  $\mu$ l binding buffer. The cells were stained with 50  $\mu$ g/ml propidium iodide at room temperature for 5 minutes, followed by flow cytometric analysis using a FACScan flow cytometer and CellQuest software (BD).

**Statistics.** Data are presented as the mean  $\pm$  SD. Differences between 2 groups were analyzed using a 2-tailed Student's *t* test and incorporated into GraphPad Prism 5 software (GraphPad Software).

*P* < 0.05 was considered statistically significant. ANOVA was used for comparisons between multiple groups.

**Study approval.** The protocol concerning the use of biopsy samples from patients with FSGS and of nephrectomized tissues was approved by the local committee on human subjects at Jinling Hospital, Nanjing University School of Medicine (2012GJJ-034). Written informed consent was provided by each patient. All animal protocols and procedures were approved by the IACUC of Jinling Hospital.

## Acknowledgments

This work was supported by grants from the National Basic Research Program of China (973 Program, 2012CB517600 and 2012CB517606); the Major International (Regional) Joint Research Project (81320108007); the Major Research Plan of the National Natural Science Foundation (91442104); and the National Natural Science Foundation of China (81370827).

Address correspondence to: Zhihong Liu, Research Institute of Nephrology, Jinling Hospital, Nanjing University School of Medicine, Nanjing, Jiangsu 210002, China. Phone: 86.25.84801992; E-mail: liuzhihong@nju.edu.cn. Or to: Shaolin Shi, Research Institute of Nephrology, Jinling Hospital, Nanjing University School of Medicine, Nanjing, Jiangsu 210002, China. Phone: 86.25.80863793; E-mail: shaolinshi1001@yahoo.com.

- Kriz W, Gretz N, Lemley KV. Progression of glomerular diseases: is the podocyte the culprit? *Kidney Int.* 1998;54(3):687–697.
- Shankland SJ. The podocyte's response to injury: role in proteinuria and glomerulosclerosis. *Kidney Int.* 2006;69(12):2131–2147.
- Schiffer M, et al. Apoptosis in podocytes induced by TGF-beta and Smad7. *J Clin Invest.* 2001;108(6):807–816.
- Shi S, et al. Podocyte-selective deletion of dicer induces proteinuria and glomerulosclerosis. *J Am Soc Nephrol.* 2008;19(11):2159–2169.
- Harvey SJ, et al. Podocyte-specific deletion of dicer alters cytoskeletal dynamics and causes glomerular disease. *J Am Soc Nephrol.* 2008;19(11):2150–2158.
- Ho J, Ng KH, Rosen S, Dostal A, Gregory RI, Kreidberg JA. Podocyte-specific loss of functional microRNAs leads to rapid glomerular and tubular injury. *J Am Soc Nephrol.* 2008;19(11):2069–2075.
- Gebeshuber CA, et al. Focal segmental glomerulosclerosis is induced by microRNA-193a and its downregulation of WT1. *Nat Med.* 2013;19(4):481–487.
- Lin CL, et al. MicroRNA-29a promotion of nephrin acetylation ameliorates hyperglycemia-induced podocyte dysfunction. *J Am Soc Nephrol.* 2014;25(8):1698–1709.
- Wu J, et al. Downregulation of microRNA-30 facilitates podocyte injury and is prevented by glucocorticoids. *J Am Soc Nephrol.* 2014;25(1):92–104.
- Shi S, et al. Smad2-dependent downregulation of miR-30 is required for TGF- $\beta$ -induced apoptosis in podocytes. *PLoS One.* 2013;8(9):e75572.
- Welsh GI, Saleem MA. The podocyte cytoskeleton — key to a functioning glomerulus in health and disease. *Nat Rev Nephrol.* 2012;8(1):14–21.
- Garg P, Holzman LB. Podocytes: gaining a foothold. *Exp Cell Res.* 2012;318(9):955–963.
- Chuang PY, He JC. Signaling in regulation of podocyte phenotypes. *Nephron Physiol.* 2009;111(2):p9–p15.
- Greka A, Mundel P. Calcium regulates podocyte actin dynamics. *Semin Nephrol.* 2012;32(4):319–326.
- Chen S, et al. Calcium entry via TRPC6 mediates albumin overload-induced endoplasmic reticulum stress and apoptosis in podocytes. *Cell Calcium.* 2011;50(6):523–529.
- Wang Y, et al. Activation of NFAT signaling in podocytes causes glomerulosclerosis. *J Am Soc Nephrol.* 2010;21(10):1657–1666.
- Wang L, Chang JH, Paik SY, Tang Y, Eisner W, Spurney RF. Calcineurin (CN) activation promotes apoptosis of glomerular podocytes both in vitro and in vivo. *Mol Endocrinol.* 2011;25(8):1376–1386.
- Kincaid R. Calmodulin-dependent protein phosphatases from microorganisms to man. *Adv Second Messenger Phosphoprotein Res.* 1993;27:1–23.
- Ueki K, Muramatsu T, Kincaid RL. Structure and expression of two isoforms of the murine calmodulin-dependent protein phosphatase regulatory subunit (calcineurin B). *Biochem Biophys Res Commun.* 1992;187(1):537–543.
- Mukai H, Chang CD, Tanaka H, Ito A, Kuno T, Tanaka C. cDNA cloning of a novel testis-specific calcineurin B-like protein. *Biochem Biophys Res Commun.* 1991;179(3):1325–1330.
- Jain J, et al. The T-cell transcription factor NFATp is a substrate for calcineurin and interacts with Fos and Jun. *Nature.* 1993;365(6444):352–355.
- Wang HG, et al. Ca<sup>2+</sup>-induced apoptosis through calcineurin dephosphorylation of BAD. *Science.* 1999;284(5412):339–343.
- Shibasaki F, Kondo E, Akagi T, McKeon F. Suppression of signalling through transcription factor NF-AT by interactions between calcineurin and Bcl-2. *Nature.* 1997;386(6626):728–731.
- Molkentin JD, et al. A calcineurin-dependent transcriptional pathway for cardiac hypertrophy. *Cell.* 1998;93(2):215–228.
- Gomez AM, Ruiz-Hurtado G, Benitah JP, Dominguez-Rodriguez A. Ca(2+) fluxes involvement in gene expression during cardiac hypertrophy. *Curr Vasc Pharmacol.* 2013;11(4):497–506.
- Xie J, Cha SK, An SW, Kuro OM, Birnbaumer L, Huang CL. Cardioprotection by Klotho through downregulation of TRPC6 channels in the mouse heart. *Nat Commun.* 2012;3:1238.
- Seo K, et al. Combined TRPC3 and TRPC6 blockade by selective small-molecule or genetic deletion inhibits pathological cardiac hypertrophy. *Proc Natl Acad Sci U S A.* 2014;111(4):1551–1556.
- Wu X, Eder P, Chang B, Molkentin JD. TRPC channels are necessary mediators of pathologic cardiac hypertrophy. *Proc Natl Acad Sci U S A.* 2010;107(15):7000–7005.
- Mukherjee A, Soto C. Role of calcineurin in neurodegeneration produced by misfolded proteins and endoplasmic reticulum stress. *Curr Opin Cell Biol.* 2011;23(2):223–230.
- Woods NK, Padmanabhan J. Neuronal calcium signaling and Alzheimer's disease. *Adv Exp Med Biol.* 2012;740:1193–1217.
- Winn MP, et al. A mutation in the TRPC6 cation channel causes familial focal segmental glomerulosclerosis. *Science.* 2005;308(5729):1801–1804.
- Dietrich A, Chubanov V, Gudermann T. Renal

- TRPathies. *J Am Soc Nephrol*. 2010;21(5):736–744.
33. Paul C, et al. The actin cytoskeleton of kidney podocytes is a direct target of the antiproteinuric effect of cyclosporine A. *Nat Med*. 2008;14(9):931–938.
  34. Muzumdar MD, Tasic B, Miyamichi K, Li L, Luo L. A global double-fluorescent Cre reporter mouse. *Genesis*. 2007;45(9):593–605.
  35. Moeller MJ, Sanden SK, Soofi A, Wiggins RC, Holzman LB. Podocyte-specific expression of cre recombinase in transgenic mice. *Genesis*. 2003;35(1):39–42.
  36. Schiffer M, et al. Inhibitory smads and tgf-Beta signaling in glomerular cells. *J Am Soc Nephrol*. 2002;13(11):2657–2666.
  37. Brukamp K, Jim B, Moeller MJ, Haase VH. Hypoxia and podocyte-specific Vhlh deletion confer risk of glomerular disease. *Am J Physiol Renal Physiol*. 2007;293(4):F1397–F1407.
  38. Kambham N, et al. Congenital focal segmental glomerulosclerosis associated with beta4 integrin mutation and epidermolysis bullosa. *Am J Kidney Dis*. 2000;36(1):190–196.
  39. Woroniecka KI, Park AS, Mohtat D, Thomas DB, Pullman JM, Susztak K. Transcriptome analysis of human diabetic kidney disease. *Diabetes*. 2011;60(9):2354–2369.
  40. Obad S, et al. Silencing of microRNA families by seed-targeting tiny LNAs. *Nat Genet*. 2011;43(4):371–378.
  41. Wei C, et al. Modification of kidney barrier function by the urokinase receptor. *Nat Med*. 2008;14(1):55–63.
  42. Yu F, Deng H, Yao H, Liu Q, Su F, Song E. Mir-30 reduction maintains self-renewal and inhibits apoptosis in breast tumor-initiating cells. *Oncogene*. 2010;29(29):4194–4204.
  43. Zhang B, et al. The calcineurin-NFAT pathway allows for urokinase receptor-mediated  $\beta$ 3 integrin signaling to cause podocyte injury. *J Mol Med (Berl)*. 2012;90(12):1407–1420.
  44. Mallipattu SK, et al. Kruppel-like factor 6 regulates mitochondrial function in the kidney. *J Clin Invest*. 2015;125(3):1347–1361.
  45. Li J, Donath S, Li Y, Qin D, Prabhakar BS, Li P. miR-30 regulates mitochondrial fission through targeting p53 and the dynamin-related protein-1 pathway. *PLoS Genet*. 2010;6(1):e1000795.
  46. Nijenhuis T, et al. Angiotensin II contributes to podocyte injury by increasing TRPC6 expression via an NFAT-mediated positive feedback signaling pathway. *Am J Pathol*. 2011;179(4):1719–1732.
  47. Liu X, et al. Attenuation of store-operated  $Ca^{2+}$  current impairs salivary gland fluid secretion in TRPC1(–/–) mice. *Proc Natl Acad Sci U S A*. 2007;104(44):17542–17547.
  48. Sonneveld R, et al. Glucose specifically regulates TRPC6 expression in the podocyte in an AngII-dependent manner. *Am J Pathol*. 2014;184(6):1715–1726.
  49. Yang H, et al. High glucose-induced apoptosis in cultured podocytes involves TRPC6-dependent calcium entry via the RhoA/ROCK pathway. *Biochem Biophys Res Commun*. 2013;434(2):394–400.
  50. Dietrich A, Fahlbusch M, Gudermann T. Classical Transient Receptor Potential 1 (TRPC1): channel or channel regulator? *Cells*. 2014;3(4):939–962.
  51. Wiggins RC. The spectrum of podocytopathies: a unifying view of glomerular diseases. *Kidney Int*. 2007;71(12):1205–1214.
  52. Ma F, et al. The microRNA miR-29 controls innate and adaptive immune responses to intracellular bacterial infection by targeting interferon-gamma. *Nat Immunol*. 2011;12(9):861–869.
  53. Wharram BL, et al. Podocyte depletion causes glomerulosclerosis: diphtheria toxin-induced podocyte depletion in rats expressing human diphtheria toxin receptor transgene. *J Am Soc Nephrol*. 2005;16(10):2941–2952.
  54. Moller CC, et al. Induction of TRPC6 channel in acquired forms of proteinuric kidney disease. *J Am Soc Nephrol*. 2007;18(1):29–36.
  55. Croce N, et al. NPY modulates miR-30a-5p and BDNF in opposite direction in an in vitro model of Alzheimer disease: a possible role in neuroprotection? *Mol Cell Biochem*. 2013;376(1–2):189–195.
  56. Mellios N, Huang HS, Grigorenko A, Rogaev E, Akbarian S. A set of differentially expressed miRNAs, including miR-30a-5p, act as post-transcriptional inhibitors of BDNF in prefrontal cortex. *Hum Mol Genet*. 2008;17(19):3030–3042.
  57. Rastaldi MP, et al. Glomerular podocytes contain neuron-like functional synaptic vesicles. *FASEB J*. 2006;20(7):976–978.
  58. Boerries M, et al. Molecular fingerprinting of the podocyte reveals novel gene and protein regulatory networks. *Kidney Int*. 2013;83(6):1052–1064.
  59. Nakamura A, Imaizumi A, Yanagawa Y, Kohsaka T, Johns EJ.  $\beta$ (2)-Adrenoceptor activation attenuates endotoxin-induced acute renal failure. *J Am Soc Nephrol*. 2004;15(2):316–325.
  60. Wang X, et al. Histone deacetylase 4 selectively contributes to podocyte injury in diabetic nephropathy. *Kidney Int*. 2014;86(4):712–725.
  61. van den Berg JG, van den Bergh Weerman MA, Assmann KJ, Weening JJ, Florquin S. Podocyte foot process effacement is not correlated with the level of proteinuria in human glomerulopathies. *Kidney Int*. 2004;66(5):1901–1906.
  62. Zhou Y, et al. Peroxisome proliferator-activated receptor-alpha is renoprotective in doxorubicin-induced glomerular injury. *Kidney Int*. 2011;79(12):1302–1311.
  63. Venkatarreddy M, et al. Estimating podocyte number and density using a single histologic section. *J Am Soc Nephrol*. 2014;25(5):1118–1129.
  64. Saleem MA, et al. A conditionally immortalized human podocyte cell line demonstrating nephrin and podocin expression. *J Am Soc Nephrol*. 2002;13(3):630–638.
  65. Grynkiewicz G, Poenie M, Tsien RY. A new generation of  $Ca^{2+}$  indicators with greatly improved fluorescence properties. *J Biol Chem*. 1985;260(6):3440–3450.
  66. Asano T, Matsusaka T, Mizutani S, Ichikawa I. Rapid downregulation of  $\beta$ -actin-based CAG promoter and filamentous actin in injured podocytes. *J Med Dent Sci*. 2005;52(2):129–134.